Université de Montréal

Molecular Networks Created by Charge-Assisted Hydrogen Bonds Between Bis(aminidinium) Cations and Carboxylates, Sulfonates, Phosphonates and Phosphates

par

Sharon Lie Chin Cheong

Département de chimie, Université de Montréal
Faculté des Arts et des Sciences

Mémoire présenté à la Faculté des Études Supérieures et Postdoctorales
en vue de l'obtention du grade de maîtrise en Chimie

Juin, 2013

Résumé

L'objectif de cette étude est d'apprendre à créer de nouveaux matériaux moléculaires par design. À l'heure actuelle, il n'existe aucune méthode générale pour la prédiction des structures et des propriétés, mais des progrès importants ont été accomplis, en particulier dans la fabrication de matériaux moléculaires ordonnés tels que des cristaux. En ces matériaux, l'organisation peut être contrôlée efficacement par la stratégie de la tectonique moléculaire. Cette approche utilise des molécules appelées "tectons", qui peuvent s'associer de manière dirigée par des interactions non covalentes prévisibles. De cette façon, la position de chaque molécule par rapport à ses voisins peut être programmée avec un degré élevé de fiabilité pour créer des cristaux et d'autres matériaux organisés avec des caractéristiques et des propriétés structurelles souhaitables. Le travail que nous allons décrire est axé sur l'utilisation de l'association des cations bis(aminidinium) avec des carboxylates, sulfonates, phosphonates et phosphates, afin de créer des réseaux moléculaires prévisibles. Ces réseaux promettent d'être particulièrement robuste, car ils sont maintenus ensemble par de multiples liaisons hydrogène assistées par des interactions électrostatiques.

Mots-clés : Matériaux moléculaires, génie cristallin, liaison hydrogène, interactions électrostatiques

Abstract

The goal of this study is to learn how to create new molecular materials by design. At present, there is no general method for predicting structures and properties, but significant progress is being made, particularly in making ordered molecular materials such as crystals. In such materials, organization can be controlled effectively by the strategy of molecular tectonics. This approach uses molecules called "tectons", which can associate in ways directed by predictable non-covalent interactions. In this way, the position of each molecule relative to its neighbors can be programmed with a high degree of reliability to create crystals and other ordered materials with desirable structural features and properties. The work that we will describe focuses on using the association of bis(aminidinium) cations with carboxylates, sulfonates, and phosphates to create predictable molecular networks. Such networks promise to be unusually robust because they are held together by multiple charge-assisted hydrogen bonds.

Keywords : Molecular materials, tectons, crystal engineering, charge-assisted hydrogen bonds

Table of Contents

2.0 CHAPTER 2:

Article 1 : Lie, S.; Maris, T.; Malveau, C.; Beaudoin, D.; Helzy, F.; Wuest, J. D. "Molecular Networks Created by Charge-Assisted Hydrogen Bonding in Carboxylate Salts of a Bis(amidine)" *Cryst. Growth Des.* **2013**, *13*, 1872-1877.

3.0 CHAPTER 3:

Article 2 : Lie, S.; Maris, T.; Wuest, J. D.

"Molecular Networks Created by Charge-Assisted Hydrogen Bonding in Phosphonate, Phosphate, and Sulfonate Salts of Bis(amidines)" *Cryst. Growth Des.* Submitted for publication.

4.0 CHAPTER 4: CONCLUSION

List of Tables

CHAPTER 2

CHAPTER 3

List of Figures

CHAPTER 1

CHAPTER 2

CHAPTER 3

List of Abbreviations

Å	Ångstrom
ºC	degree Celsius
δ	chemical shift
Calcd	calculated
Dec	decomposition
DMSO	dimethyl sulfoxide
EtOH	ethanol
ESI-MS	electrospray ionization mass spectrometry
FTIR	Fourier-transform infrared
Hz	Hertz
Kcal	kilocalorie
kJ	kilojoule
m	multiplet
m/*e*	mass per unit charge
MHz	megahertz
Mol	mole
m.p.	melting point
NMR	nuclear magnetic resonance
s	singlet

To my family

Acknowledgments

My gratitude goes, first of all, to my supervisor, Professor Wuest, for the opportunity of doing research in his group. His trust and kind words are what allowed me to regain my self-confidence in academia.

This mémoire would not have been possible without the contribution of various coworkers; I would like to thank most particularly Thierry Maris, Daniel Beaudoin, and Hui Zhou for their precious advices and for being role models with regards to conducting research. I have greatly benefited from their expertise in the areas of crystallography, organic synthesis and STM. My acknowledgements also go to various departmental personnel for their help and availability at all instances. I would like to thank the members of the NMR Regional Laboratory team, particularly Cédric Malveau; the Centre for Mass Spectral Analysis, and the Centre for Elemental Analysis. Much gratitude is also given to Mildred Bien-Aimé for administrative aid and numerous friendly conversations.

I would never have been able to go through my graduate studies without the support of my family. I am grateful to my parents and Fifi for their unconditional love and encouragement. I highly appreciate the support offered by my brother Wesley who has been present throughout my good and bad times. A special thought goes to François, who helped in the correction of this mémoire and whom I had the opportunity to meet during my graduate studies. Finally I would like to express my gratitude to all my relatives, specially my grandmother and my aunt Lily, without whom this journey would never have been possible.

1.0 Chapter 1: Introduction

1.1. Supramolecular Chemistry

Traditional molecular chemistry focuses on structures held together by covalent bonds. A newer area of molecular science, often referred to as "chemistry beyond the molecule",[1] is the field of supramolecular chemistry. Whereas traditional chemistry builds molecules through manipulation of the covalent bond, supramolecular chemistry focuses on using non-covalent intermolecular interactions as a tool for generating new molecular entities with well-defined features.[2]

To an important extent, supramolecular chemistry is inspired by the biological world, because non-covalent interactions play key roles in many biological systems.[3] For example, strands of nucleic acids are linked specifically by weak interactions to define genetic makeup and convey information that directs the functions of living things. Highly specific intermolecular interactions also play a central role in the binding of substrates to enzymes, in directing drugs to their targets, and in determining the behaviour of protein assemblies that govern the propagation of signals between cells. As a result, the study of these interactions is a crucially important undertaking, both as a source of information about how complex natural systems work and as a foundation for applying weak interactions in new ways.[4] It would be tremendously difficult to build single giant molecules that could carry out the necessary biological processes, using only linear syntheses based on the construction of covalent bonds. Supramolecular chemistry plays a dominant role in biological organization because it offers advantages over conventional molecular chemistry. These advantages include (1) a decrease in

structural errors due to reversible selection of subunits during the self-assembling process, which allows errors to be corrected; (2) ease of formation of the end product, because non-covalent interactions are formed rapidly; and (3) synthetic economy resulting from the fact that in molecular association, all of the atoms of the starting components appear in the self-assembled structure.[5] These multiple advantages can be extended and applied to many other systems, which is why supramolecular chemistry has continued to expand in importance in recent years.

Through its success in creating complex systems by manipulating interactions between the components, supramolecular chemistry intersects the science of molecular information.[6] Information stored at the molecular level is transferred and processed at the supramolecular level through molecular recognition operating by means of specific interactions. The impact of supramolecular chemistry has grown rapidly in recent decades, and the field has gained a position of prominence as the science of informed matter at the interfaces of biology and physics (Figure 1).[4,7] In general, supramolecular science points towards the discovery and implementation of new rules that will ultimately meet the challenge of creating new forms of complex matter.[7]

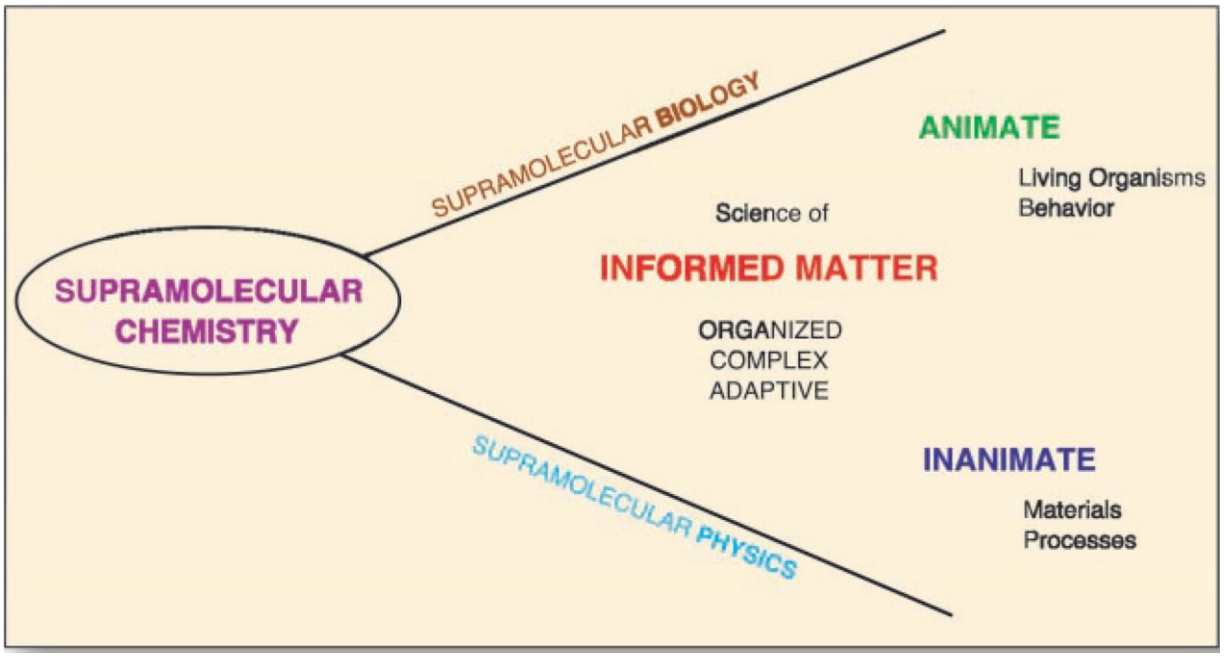

Figure 1. Supramolecular science as the science of informed matter at the interfaces of chemistry with biology and physics.[4]

1.2 Crystal Engineering

There are many important manifestations of supramolecular chemistry outside the realm of biology. One of the most striking is the phenomenon of molecular recognition that takes place in the formation and growth of crystals. In fact, Dunitz defines the crystal as "the supramolecule par excellence."[8] Crystals can be considered to be the ultimate supermolecules, and their structure shows how solid-state molecular recognition can lead to the assembly of countless individual molecules, all held together by non-covalent interactions under the influence of chemical and geometrical factors.[9,10]

One of the goals of crystal engineering is to provide "understanding of intermolecular interactions in the context of crystal packing…" and to lead to the "utilisation of such understanding in the design of new solids with desired physical and chemical properties."[11] Crystal engineering is a cross-disciplinary field and lies at the intersection of many important domains, including chemistry, crystallography, and materials science. Like supramolecular chemistry in solution, crystal engineering is governed by basic principles of molecular recognition, applied to chemical events occurring in the solid state. Purposeful molecular recognition is commonly referred to as supramolecular chemistry in solution and as crystal engineering when it occurs in the solid state.[11-13]

Molecules in the interior of a solid are closely surrounded by multiple neighbors, all of which interact in various ways. In this way, it is possible to see molecular solids as the product of a

series of steps of recognition processes in which each component is positioned relative to its neighbors. The resulting construction of molecular networks held together by covalent interactions can be considered to be part of the foundation of crystal engineering. Molecular networks can be defined as assemblies held together by specific patterns of interaction, which repeat through space. The individual components can be viewed as consisting of a core that defines the molecular geometry and other properties, along with peripheral sites of molecular recognition that control organization. The type of network formed depends on the number of sites of strong association attached to the molecular core. Two such sites will give rise to one-dimensional networks (α-networks), whereas two or three sites will result in two-dimensional (β) and three-dimension (γ) networks, respectively.[14]

To be able to control molecular organization in the solid state, complete understanding of the intermolecular interactions between the particular components has to be achieved. Much of our understanding of these interactions is based on structural analyses using X-ray crystallography, which is the analytical technique of choice for revealing the details of non-covalent intermolecular interactions governing the three-dimensional molecular assembly in crystals.[15-17] However, despite broad understanding of these interactions and vast amounts of structural data, there is still no general method for predicting the collective behavior of molecules in detail, such as how they will crystallize. Nevertheless, the field is under very active investigation, and rapid progress is being made in controlling molecular organization in crystals.[18-21]

A major preoccupation of crystal engineering is learning how to produce predictably ordered structures that have specific desired properties.[15] In principle, controlling the properties of solids can be achieved by building them from suitably chosen molecular components that associate predictably to form programmed three-dimensional structures. The overall result can be described as the translation of structural design (at the molecular level) to property design (in the final bulk material). For this reason, the field of crystal engineering has attracted growing attention, owing to its potential for helping to reveal how technologically important new materials can be designed.[16] The new concepts developed so far have already proved to be of great significance in particular areas, such as in the synthesis of porous solids, clay-like materials and ion-exchange materials for the purpose of separations and catalysis. Moreover, the investigation of the application of these new strategies for the design of novel optical, electronic and magnetic materials based on molecular components is currently an active field of study.[15] Rapid progress in the discovery of new functional materials can be expected to occur in the coming years, in large part because of the contributions of modern crystal engineering.

1.3 Molecular Tectonics

Non-covalent intermolecular interactions are of utmost importance in crystal engineering because they provide the means for controlling the organization of molecules in the solid state.[22] An effective strategy for engineering crystals is to build them from molecules that possess well-defined geometries and are able to engage in multiple intermolecular interactions according to reliable motifs of association.[23,24] With the combined effect of geometry and interaction, the organization of molecules can be properly directed, and the position of each subunit relative to its neighbors can be programmed with a high degree of reliability, thus making it possible to engineer crystals and other ordered materials with desirable structural features and properties.

This approach is sometimes called *molecular tectonics*, which uses molecules called *tectons* that can associate in ways directed by predictable non-covalent interactions.[25,26] The word "tecton" is derived from the Greek word for builder, and it refers to molecules of defined topology whose interactions are governed by specific attractive forces that provide the driving force for assembly. Correspondingly, "molecular tectonics" is defined as being the art and science of supramolecular construction using tectonic subunits.[26] These terms are illustrated by the schematic assembly shown in Figure 2.

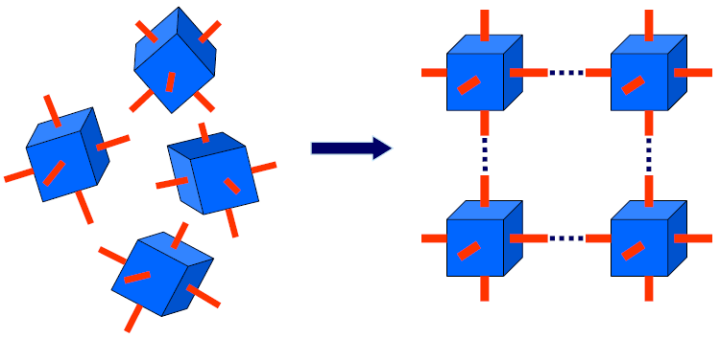

Figure 2. Schematic representation of tectons self-assembling to form a network.[4]

1.4 Hydrogen Bonds

A hydrogen bond, which can be represented by the broken line in the structure X-H···A, is an interaction wherein a hydrogen atom is attracted to two atoms, X and A, rather than just one. In this way, the hydrogen bond acts like a bridge between the two atoms.[27] An early definition stated that a hydrogen bond exists if there is evidence of a bond, and if there is evidence that the bond sterically involves a hydrogen atom already bonded to another atom.[28] A limitation of this definition is that it also includes van der Waals contacts and three-center two-electron interactions. Therefore, a more modern definition would state that "an X-H···A interaction is called a hydrogen bond if it constitutes a local bond and X- H acts as proton donor to A."[29] In a hydrogen bond X-H···A, the group X-H is called the donor and A is called the acceptor. The bond dissociation energies of hydrogen bonds range from 0.2 to 40 kcal mol^{-1}, and the type and function of a specific hydrogen bond depends on where its strength lies within this range.[29]

Many types of non-covalent intermolecular interactions can be used to control the organization of tectons; however, among all of the possibilities, the hydrogen bond remains the most exploited. In part, this is because it is strong enough to ensure association while still allowing association to be reversible so that errors of assembly can be corrected. In addition, the directionality of the bond allows the geometry of the resulting molecular assemblies to be predicted with confidence.[26] The hydrogen bond can be considered to be the most important of all directional intermolecular interactions.[29] It is a determinant factor in controlling molecular conformation and aggregation. Furthermore, a vast number of chemical and biological systems

cannot operate without the presence of hydrogen bonding. The defining role of hydrogen bonding in determining the structure and properties of many compounds and systems reflects its importance. Its properties can be used in combination with organic synthesis to direct molecular assembly in solid-state chemistry. For this reason, hydrogen bonding has been used extensively in the building of molecular networks.[29-31] Moreover, the strength of hydrogen bonds can be modulated according to need, by altering the polarity of the groups involved or by introducing the effects of charge, resonance or cooperative assistance.[32-33]

1.5 Charge-Assisted Hydrogen Bonds

An interesting way to increase the strength of interactions is based on the simultaneous use of hydrogen bonding and less directional electrostatic interactions between complementary units, giving rise to 'charge-assisted hydrogen bonds' (CAHBs). These bonds consist of donors and acceptors with an ionic character that reinforces the electrostatic dipole-dipole character of the hydrogen bond, thus positioning them among the strongest types of hydrogen bonds. Most CAHBs have a strength that falls at least in the middle of the 1 $kJmol^{-1}$ (weak) to >155 $kJmol^{-1}$ (extremely strong) range of hydrogen-bond strengths.[31] Thus, CAHBs are strong hydrogen bonds and have been referred to as ionic, positive- or negative-ion, or low-barrier hydrogen bonds.[34] Similarly, they have also been classified in crystals according to whether they are positive charge-assisted, negative charge-assisted, or resonance-assisted.[35]

In the past few years, the impact of CAHBs in the field of crystal engineering has known a substantial increase, and they have shown great effectiveness in the design of molecular networks. It has been proven that CAHBs provide a means of introducing robustness to networks due to a combination of stronger intermolecular forces between the molecular entities. Those strong interactions, when used in molecules with suitable structures, allow the design of organic solid-state materials with a high degree of rational control.[31]

There are numerous examples showing fascinating crystal architectures, in which the assembly is directed by CAHBs. Two of the most common and robust types of such bonds encountered are the $^{+}N–H\cdots O^{-}$ and $^{+}N–H\cdots N^{-}$ hydrogen bonds. Previous studies have revealed that N–H

donors carrying a positive charge give rise to shorter bonds than uncharged N–H groups, and that carboxylate anions are stronger acceptors than uncharged species such as amides, ketones, and carboxyls.[31] Theoretical aspects of CAHBs, as well as of other types of hydrogen bonds, have been reviewed recently.[36]

Overall, it is evident that the outstanding properties associated with CAHBs makes them of great significance in the systematic construction of molecular networks. Their presence allows a better control of molecular assembly leading to materials with new solid-state properties.

1.6 Molecular Networks Created by Charge-Assisted Hydrogen Bonds Between Bis(aminidinium) Cations and Oxygenate Anions

The reaction of suitable acids with bases leading to the formation of crystalline salts provides a simple strategy for incorporating charge-assisted hydrogen bonds in structures. Amidines (Figure 3) are tectons of potential interest because the protonated amidinium cation can be used to form charge-assisted hydrogen bonds with various anions.

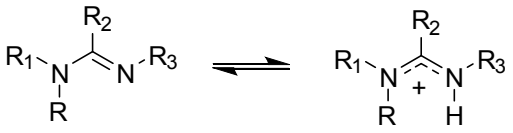

Figure 3. Basic structure of an amidine and an amidinium cation.

The structure of the ion pairs can be better controlled in instances where each atom of nitrogen of the amidinium cation is protonated, thus allowing it to donate multiple hydrogen bonds in order to form cyclic pairs with diverse anions. It is for this reason that, among all the multitude of potential CAHB donors available, amidinium cations are among the most attractive.

Although simple amidinium cations can form complex extended hydrogen-bonded networks, bis(amidinium) dications offer an increased possibility of forming strong cyclic pairs with two dianions, thereby yielding chains linked in two directions by multiple CAHBs (Figure 4). The building blocks needed for such a construction would consist of an organic core to which two

amidinium groups are attached and are available for forming hydrogen-bonded networks with a variety of different complementary anionic acceptors.[32,37-38]

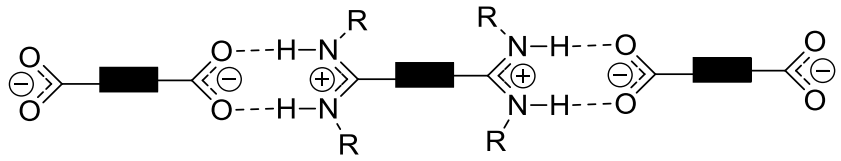

Figure 4. Cyclic charge-assisted hydrogen-bonding motif between a bis(amidinium) dication and two dianions.

Flexible acyclic amidinium units do not allow the orientation of the N-H donor sites to be controlled predictably, but the use of suitable cyclic derivations reduces uncertainty about the geometry of the cation.[39] This strategy can be put into practice by treating suitable cyclic bis(amidines) with diacids such as dicarboxylic acids, leading to the formation of salts that can form hydrogen-bonded rings or chains. In principle, this approach can be extended to the potential formation of more intricate networks created from molecules with multiple amidine and carboxyl groups. Indeed, there are already initial reports of charge-assisted hydrogen-bonded networks between bis(amidinium) cations and diverse carboxylates.[39-49]

Interactions of bis(amidinium) cations with dicarboxylates can be expected to give rise to the formation of one-dimensional networks. It is clear that to form sheets, the components will have to be modified so that basic rings and chains are interconnected. Modification of the assembling units by the addition of another dimension provides a means of achieving this

extension. For example, use of a trigonal acceptor might be expected to produce anionic sheets held together by multiple CAHBs.[50] In these ways, bis(amidinium) cations can be combined with with a variety of anions to create predictable molecular networks held together by strong hydrogen bonds. Work of this type can be expected to reveal how CAHBs can serve as powerful tools in crystal design. Their combination of strength and versatility opens the door to effective new strategies for engineering complex molecular networks.[31]

1.7 Purpose of the Study

Molecular tectonics is an effective strategy for the rational construction of molecular materials. The strategy relies on the use of strong directional intermolecular interactions to control how neighboring components are positioned. Previous work has established the effectiveness of hydrogen bonds, particularly those strengthened by additional electrostatic attraction (CAHBs). The work we have carried out focuses on the use of CAHBs formed by cations derived from bis(amidines), which have features expected to lead to the creation of robust molecular networks. Our initial study was inspired by earlier work of Hosseini and collaborators, who have reported structures derived from various bis(amidines) and acids. Their work revealed how the choice of appropriate cyclic amidinium units can ensure proper orientation of the N–H groups, thereby exerting better control over the geometry of the cation and the structure of the resulting network. Our goal has been to extend this strategy by using new bis(amidines), together with various complex acids (carboxylic, sulfonic, and phosphonic) expected to form amidinium salts that generate complex networks held together by multiple CAHBs. Our findings have shed light on the ability of multiple CAHBs to produce robust molecular materials with predictable structures. Ultimately, our results will provide a deeper understanding of how specific molecules and interactions can be used to create new materials by design.

1.8 References

1. Lehn, J.-M. *Supramolecular Chemistry: Concepts and Perspectives*. VCH: Weinheim; New York, 1995.
2. Lehn, J.-M. *Science* **1993**, 260, 1762-1763.
3. Whitesides, G. M.; Mathias, J. P.; Seto, C. T. *Science* **1991**, 254, 1312-1319.
4. Lehn, J.-M. *Science* **2002**, 295, 2400-2403.
5. Lawrence, D. S.; Jiang, T.; Levett, M. *Chem. Rev.* **1995**, 95, 2229-2260.
6. Lehn, J.-M. *Rep. Prog. Phys.* **2004**, 67, 249–265.
7. Lehn, J.-M. *Proc. Nat. Acad. Sci. USA,* **2002**, 99, 8, 4763-4768.
8. Dunitz, J. D. *Pure Appl. Chem.* **1991**, 63, 177-185.
9. *The Crystal as a Supramolecular Entity*, ed. G. R. Desiraju, Perspectives in Supramolecular Chemistry 2, Wiley, Chichester, 1996.
10. Desiraju, G. R. *Angew. Chem., Int. Ed.* **1995**, 34, 2311-2327.
11. Desiraju, G. R. *Crystal Engineering: The Design of Organic Solids*. Elsevier: Amsterdam; New York, 1989.
12. Nangia, A. *J. Chem. Sci.* **2010**, 122, 295-310.
13. Schmidt, G. M. *Pure Appl. Chem.* **1971**, 27, 647-678.
14. Fowler, F. W.; Lauher, J. W. *J. Am. Chem. Soc.* **1993**, 115, 5991-6000
15. Desiraju, G. R. *J. Mol. Struct.* **2003**, 656, 5–15.
16. Evans, O. R.; Lin, W. *Acc. Chem. Res.* **2002**, 35, 511-522.
17. Brammer, L. *Chem. Soc. Rev.* **2004**, 33, 476-489.

18. Dunitz, J. D. *Chem. Commun.* **2003**, 545-548.

19. Desiraju, G. R. *Nature Materials* **2002**, *1*, 77-79.

20. Gavezzotti, A. *Acc. Chem. Res.* **1994**, *27*, 309-314.

21. Maddox, J. *Nature* **1988**, *335*, 201.

22. Burrows, A. D. *Struct. Bond*. **2004**, 108, 55-96.

23. Wuest, J. D. *Chem. Commun.* **2005**, 5830-5837.

24. Hosseini, M. W. *Acc. Chem. Res.* **2005**, *38*, 313-323.

25. Simard, M.; Su, D.; Wuest, J. D. *J. Am. Chem. Soc.* **1991**, 113, 4696-4698

26. Su, D.; Wang, X.; Simard, M.; Wuest, J. D. *Supramol. Chem.* **1995**, 6, 171.

27. Desiraju, G. R. *Acc. Chem. Res.* **2002**, 35, 565-573.

28. Pimentel, G. C.; McClellan, A. L. *The Hydrogen Bond*. Freeman: San Francisco, 1960.

29. Steiner, T. *Angew. Chem., Int. Ed.* **2002**, 41, 48-76.

30. Emsley, J. *Chem. Soc. Rev.* **1980**, 9, 91-124.

31. Ward, M. D. *Struct. Bond.* **2009**, 132, 1-23.

32. Taylor, R.; Kennard, O. *Acc. Chem. Res.* **1984**, 17, 320-326.

33. Taylor, R.; Kennard, O.; Versichel, W. *Acta Crystallogr*. **1984**, B40, 280-288.

34. Jeffrey, G. A. *An Introduction to Hydrogen Bonding*. Oxford University Press: New York, 1997.

35. Gilli, P.; Bertolasi, V.; Ferretti, V.; Gilli, G. *J. Am. Chem. Soc.* **1994**, 116, 909-915.

36. Grabowski, S. J. *Annu. Rep. Prog. Chem., Sect C* **2006**, 102, 131-165.

37. Felix, O.; Hosseini, M. W.; De Cian, A.; Fischer, J. *New J. Chem.* **1998**, 12, 1389-1393.

38. Ferlay, S.; Bulach, V.; Felix, O.; Hosseini, M. W.; Planeix, J-M.; Kyritsakas, N. *Cryst Eng. Commun.* **2002**, 4, 447-453.

39. Hosseini, M. W. *Coord. Chem. Rev*. **2003**, 240, 157-166.

40. Stokes, F. A.; Coles, M. P.; Hitchcock, P. B. *CrystEngComm* **2012**, *14*, 771-773.

41. Han, J.; Zang, S.-Q.; Mak, T. C. W. *Chem. Eur. J.* **2010**, *16*, 5078-5088.

42. Yashima, E.; Maeda, K.; Iida, H.; Furusho, Y.; Nagai, K. *Chem. Rev.* **2009**, *109*, 6102-6211.

43. Reece, S. Y.; Nocera, D. G. *Annu. Rev. Biochem.* **2009**, *78*, 673-699.

44. Ferretti, V.; Bertolasi, V.; Pretto, L. *New J. Chem*. **2004**, 28, 646-651.

45. Corbellini, F.; Di Costanzo, L.; Crego-Calama, M.; Geremia, S.; Reinhoudt, D. N. *J. Am. Chem. Soc.* **2003**, *125*, 9946-9947.

46. Yang, J.; Melendez, R.; Geib, S. J.; Hamilton, A. D. *Struct. Chem.* **1999**, *10*, 221-228.

47. Terfort, A.; von Kiedrowski, G. *Angew. Chem., Int. Ed.* **1992**, *31*, 654-656.

48. Krechl, J.; Smrčková, S.; Pavlíková, F.; Kuthan, J. *Coll. Czech. Chem. Commun.* **1989**, *54*, 2415-2424.

49. Kraft, A. *J. Chem. Soc., Perkin Trans. 1* **1999**, 705-714.

50. Hosseini, M. W.; Brand, G.; Schanffer, P.; Ruppert, R.; De Cian, A.; Fischer, J. *Tetrahedron Lett.* **1996**, 37, 1405-1408.

2.0 Chapter 2 : Article 1

Lie, S.; Maris, T.; Malveau, C.; Beaudoin, D.; Helzy, F.; Wuest, J. D.

"Molecular Networks Created by Charge-Assisted Hydrogen Bonding in Carboxylate Salts of a Bis(amidine*)" Cryst. Growth Des.* **2013**, *13*, 1872-1877.

2.1 Introduction

Molecular tectonics provides an effective modular strategy for constructing new materials. It is governed by the self-assembly of molecules with distinct geometries which recognize themselves by means of intermolecular interactions. The application of this strategy results in a high level of predictability in molecular organization, which represents a prerequisite for engineering molecular materials.

Molecular tectonics takes advantage of a wide variety of interactions to control how adjacent modules are positioned. Of these interactions, hydrogen bonds are among the most effective. Previously reported molecular networks are typically held together by nonionic hydrogen bonds. However, strengthened association can be achieved by using charge-assisted hydrogen bonds formed by modules that have opposing charges. Previous work has identified amidinium cations as particularly effective participants in charge-assisted hydrogen bonds (CAHBs), and we have explored new facets of their use as the cationic components of extended hydrogen-bonded networks formed with carboxylate anions.

Chapter 2, presented in the form of an article, summarizes the association of bis(aminidinium) cations of 2,2'-bi-2-imidazoline with different carboxylates. These salts form extended networks in which the components are held together by multiple CAHBs. Due to the presence of charged interacting species, the resulting molecular materials have enhanced robustness.

Molecular Networks Created by Charge-Assisted Hydrogen Bonding in Carboxylate Salts of a Bis(amidine)

Sharon Lie, Thierry Maris, Cédric Malveau, Daniel Beaudoin, Fatima Helzy, and James D. Wuest*

Département de Chimie, Université de Montréal, Montréal, Québec H3C 3J7 Canada

2.2 Abstract

Amidines can be protonated by carboxylic acids to give amidinium carboxylates, and the ions can associate by forming multiple charge-assisted hydrogen bonds according to reliable motifs. Extended hydrogen-bonded networks can be constructed by treating suitable bis(amidines) with acids containing multiple carboxyl groups. To further explore the potential of this strategy, we have determined the structures of salts produced by treating 2,2'-bi-2-imidazoline, a cyclic bis(amidine), with oxalic, fumaric, terephthalic, and trimesic acids. The structures of the salts proved to incorporate features resulting predictably from the geometry of the ions and their ability to engage in charge-assisted hydrogen bonds.

2.3 Introduction

In recent years, an intensive effort has been made to learn how to create new molecular materials by design. At present, there is still no general method for predicting the collective behavior of molecules in detail,[1-4] but significant progress is being made in certain areas, such as in controlling molecular organization in crystals. A particularly effective strategy for engineering crystals is to build them from molecules that have well-defined geometries and can engage in multiple intermolecular interactions according to reliable motifs of association.[5-6] When geometries and interactions are designed to act in synergy to direct organization, the position of each molecule relative to its neighbors can be programmed with a high degree of reliability, making it possible to engineer crystals and other ordered materials with desirable structural features and properties.

Many types of non-covalent interactions can be used to ensure proper intermolecular cohesion and orientation, but hydrogen bonds stand out for their high strength and directionality. The inherent strength can be increased by polarizing the groups involved and by introducing charge, resonance, or cooperative effects.[7-8] A promising approach is based on the simultaneous use of hydrogen bonds and less directional electrostatic interactions between molecules, which can be combined to give rise to charge-assisted hydrogen bonds.[9] Such bonds offer a powerful way to make materials more robust by strengthening interactions between the molecular subunits. A simple strategy for incorporating charge-assisted hydrogen bonds in structures is to mix suitable acids and bases that react to form crystalline salts.

Amidines have been widely exploited in this way, both in biology and chemistry, because they can be protonated to form the corresponding amidinium cations (eq 1), which can then engage in charge-assisted hydrogen bonds with diverse anions.

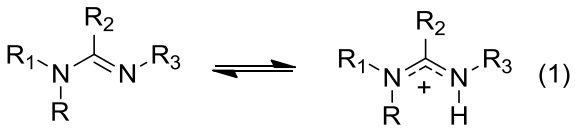

(1)

Optimal control of the structure of the ion pairs can be achieved by using amidinium salts in which each atom of nitrogen is protonated. This allows the cation to serve as a multiple donor of hydrogen bonds and to form cyclic pairs with carboxylates and their relatives according to the graph set $\mathbf{R_2^2(8)}$,[10] as shown in Figure 1.[11-21] In such ways, salts of bis(amidines) with dicarboxylic acids can give rise to hydrogen-bonded rings or chains, and more intricate networks can be created from molecules with multiple amidine and carboxyl groups. Use of appropriate cyclic amidinium units can ensure that the N–H groups will be oriented predictably, thereby eliminating uncertainty about the geometry of the cation. Elegant use of this strategy has been made by Hosseini and coworkers.[11]

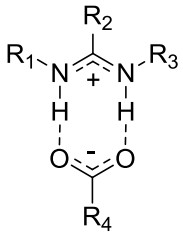

Figure 1. Cyclic charge-assisted hydrogen bonding according to graph set $\mathbf{R_2^2(8)}$ in simple amidinium carboxylates.

The present paper describes how molecular networks with predictable structural features can be assembled by combining 2,2'-bi-2-imidazoline (**BI**),[22] a cyclic bis(amidine), with oxalic (**OA**/H_2), fumaric (**FA**/H_2), terephthalic (**TA**/H_2), and trimesic acids (**TMA**/H_3), which are shown in Figure 2 along with protonated forms of bis(amidine) **BI**. If the diprotonated dicationic form **BI**/H_2^{+2} is produced under these conditions, it can serve as a donor of four N-H···acceptor hydrogen bonds. When combined with suitable carboxylates, the dication would then be expected to generate networks held together by multiple charge-assisted hydrogen bonds.

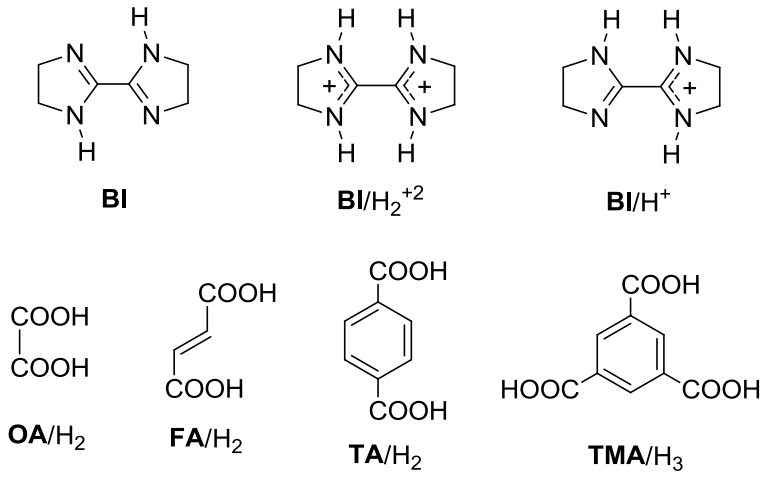

Figure 2. Molecules used to construct networks held together by multiple charge-assisted hydrogen bonds.

The structures of salts of bis(amidine) **BI** with the four carboxylic acids in Figure 2 confirm that a variety of molecular networks can be assembled by using hydrogen bonds and electrostatic interactions in combination. The relative importance of these interactions in the

observed structures depends in part on the different pK_a values of the reacting species, which determine the extent of proton transfer from the acids to bis(amidine) **BI**.[23]

2.4 Results and Discussion

2,2'-Bi-2-imidazoline (**BI**) was prepared by a published method[22] and combined in DMSO with carboxylic acids **OA**/H_2, **FA**/H_2, **TA**/H_2, and **TMA**/H_3 in various ratios. Under these conditions, bis(amidine) **BI** reacted with the acids to give salts, as a result of the large differences in pK_a between those of typical imidazolinium cations (10-11)[21,24-26] and those corresponding to the first ionizations of acids **OA**/H_2 (1.23), **FA**/H_2 (3.02), **TA**/H_2 (3.51), and **TMA**/H_3 (3.12).[27-28] Single crystals of salts were obtained by slowly cooling solutions in hot DMSO, and the structures were subsequently resolved by X-ray diffraction to reveal the composition of the salts and the nature of the interionic interactions.

2,2'-Bi-2-imidazolinium oxalate (BI/H_2^{+2}) (OA^{-2}). Mixing bis(amidine) **BI** and oxalic acid (**OA**/H_2) in a 1:1 molar ratio gave rise to crystals of composition (**BI**/H_2^{+2}) (OA^{-2}). The structure was determined by X-ray diffraction, and crystallographic parameters are summarized in Table 1. Analysis revealed the formation of tapes built from an alternating arrangement of doubly protonated biimidazolinium dications (**BI**/H_2^{+2}) and oxalate dianions (OA^{-2}), interconnected by charge-assisted hydrogen bonds according to graph set $\mathbf{R_2^2(9)}$ (Figure 3). Adjacent tapes pack closely to form sheets, which then stack to form the observed structure. Clear evidence for the full transfer of two protons from oxalic acid to bis(amidine)

BI was provided by the observation of two equal C-O bond lengths and two equal C-N bond lengths within each $\mathbf{R_2^2(9)}$ motif.

Table 1. Crystallographic data for salts (**BI**/H_2^{+2}) (**OA**$^{-2}$), (**BI**/H^+)$_2$ (**FA**$^{-2}$) • 4H_2O, (**BI**/H^+)$_2$ (**TA**^{2}), and (**BI**/H^+)$_2$ (**TMA**/H^{-2}) • H_2O.

salt	(**BI**/H_2^{+2}) (**OA**$^{-2}$)	(**BI**/H^+)$_2$ (**FA**$^{-2}$) • 4H_2O	(**BI**/H^+)$_2$ (**TA**$^{-2}$)	(**BI**/H^+)$_2$ (**TMA**/H^{-2}) • H_2O
crystallization medium	DMSO	DMSO	DMSO	DMSO
formula	$C_8H_{12}N_4O_4$	$C_{16}H_{34}N_8O_8$	$C_{20}H_{28}N_8O_4$	$C_{21}H_{30}N_8O_7$
crystal system	monoclinic	monoclinic	monoclinic	orthorhombic
space group	*C*2/*c*	*P*2$_1$/*n*	*C*2/*c*	*Pbca*
a (Å)	13.8325(6)	6.9051(3)	14.7306(4)	18.2469(6)
b (Å)	10.0215(5)	17.6822(8)	19.4915(5)	13.1870(5)
c (Å)	7.2137(3)	9.3199(4)	8.2614(2)	18.6203(6)
α (°)	90	90	90	90
β (°)	112.385(2)	109.521(2)	123.237(1)	90
γ (°)	90	90	90	90
V (Å^3)	924.63(7)	1027.53(8)	1983.99(9)	4480.5(3)
Z	4	2	4	8
T (K)	150	150	150	150
ρ_{calc} (g cm^{-3})	1.639	1.438	1.418	1.496
μ (mm^{-1})	1.140	0.984	0.89	0.967
crystal size (mm)	0.14 × 0.12 × 0.10	0.18 × 0.15 × 0.10	0.13 × 0.13 × 0.05	0.15 × 0.06 × 0.05
θ range (°)	5.61-69.92	5.62-70.04	4.24-69.43	4.75-70.07
measured reflections	8614	22246	19916	94678
independent reflections	866	2024	1851	4235
R_1, $I > 2\sigma(I)$	0.0355	0.0373	0.0388	0.0453
R_1, all data	0.0358	0.0376	0.0419	0.048
wR_2, $I > 2\sigma(I)$	0.1059	0.1064	0.1103	0.1164
wR_2, all data	0.1064	0.1068	0.1139	0.1184
GoF	1.037	1.055	1.077	1.103

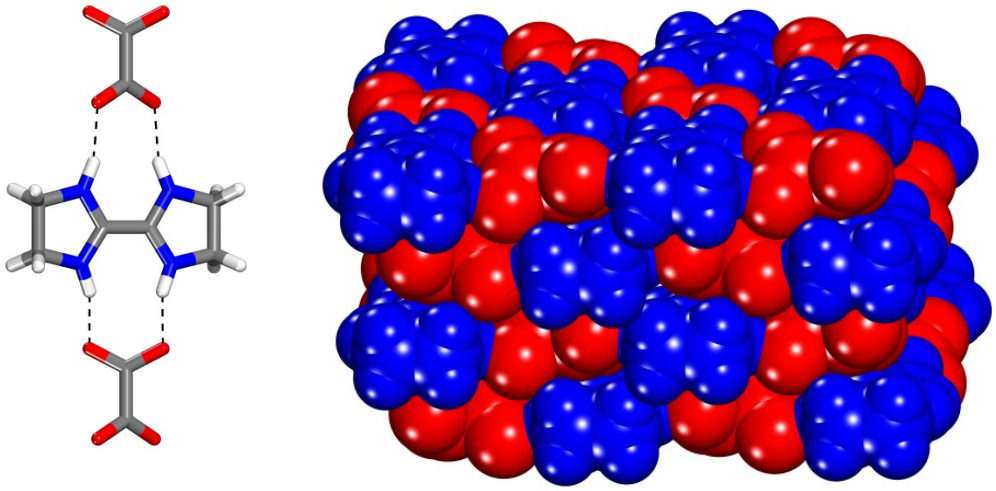

Figure 3. Representations of the structure of crystals of 2,2'-bi-2-imidazolinium oxalate salt (**BI**/H_2^{+2}) (**OA**$^{-2}$) grown from DMSO. (a) View of part of an alternating hydrogen-bonded tape composed of 2,2'-bi-2-imidazolinium dications (**BI**/H_2^{+2}) and oxalate dianions (**OA**$^{-2}$). Atoms of carbon are shown in gray, hydrogen in white, nitrogen in blue, and oxygen in red. Hydrogen bonds are shown as broken lines. (b) Side view of the tapes, showing how they pack to form sheets and how the sheets stack to form the observed structure. Biimidazolinium dications are shown in blue and oxalate dianions in red.

Detailed examination of the structure showed that the dicationic and dianionic units are connected by N-H···O hydrogen bonds with a short average N···O distance of 2.65 Å. This is shorter than the N···O distances normally observed in N···H-O hydrogen bonds (2.85 Å) formed when carboxylic acids co-crystallize with amines to form complexes without full proton transfer.[29-30] This observation provides direct evidence that hydrogen bonding in the salt (**BI**/H_2^{+2}) (**OA**$^{-2}$) is in fact charge-assisted. Within each amidinium group of the

biimidazolinium dication, the two C-N distances are nearly equal (1.315 and 1.308 Å), confirming that the compound **BI** has been doubly protonated to give an essentially symmetric structure. In contrast, the corresponding distances in the neutral bis(amidine) **BI** itself are distinctly different (1.344 and 1.284 Å).[31] Formation of a structure incorporating symmetric doubly protonated biimidazolinium dications and oxalate dianions is also confirmed by the solid-state ^{1}H spectrum of the crystalline salt, which shows only two signals derived from the dication. Few hydrogen-bonded structures corresponding to the graph set $\mathbf{R_2^2(9)}$ have been reported.[32-34] The geometry of the ring shows little evidence of strain; in particular, the N-H···O angles are nearly linear (average of 162°), and the dihedral angle between the two imidazolinium rings is only 7.4°.

2,2'-Bi-2-imidazolinium fumarate ($\mathbf{BI/H^+)_2}$ ($\mathbf{FA^{-2}}$) • $\mathbf{4H_2O}$. Mixing bis(amidine) **BI** and fumaric acid (**FA**/H_2) in a 1:1 molar ratio in DMSO gave crystals that proved to be a tetrahydrated form of a 2:1 salt of biimidazolinium monocation **BI**/H^+ and fumarate dianion ($\mathbf{FA}^{-2}$). Structural analysis (see Table 1 for crystallographic parameters) again revealed the formation of tapes held together by charge-assisted hydrogen bonds. However, double protonation of bis(amidine) **BI** did not occur, possibly because fumaric acid has a higher pK_a than oxalic acid. Instead, the tapes were found to consist of an alternating arrangement of fumarate dianions and dimers of the biimidazolinium monocation (Figure 4). As in the oxalate salt, each carboxylate group of fumarate accepts two hydrogen bonds from a biimidazolinium monocation to form a characteristic nine-membered ring corresponding to graph set $\mathbf{R_2^2(9)}$, and the fumarate dianions are also hydrogen-bonded to water. Inter-tape hydrogen bonds

involving water link the tapes into corrugated sheets, and the sheets are connected by additional hydrogen bonds to water.

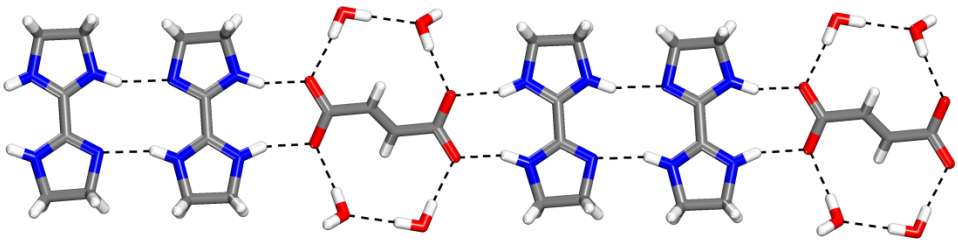

a

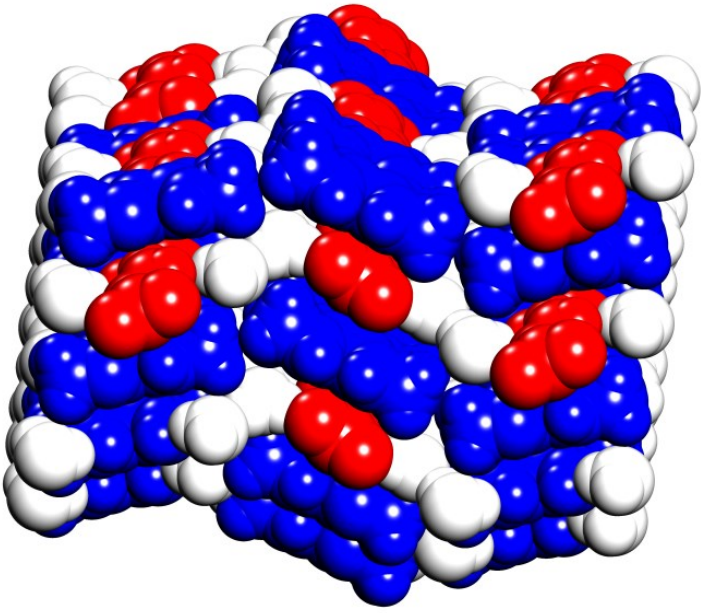

b

Figure 4. Representation of the structure of crystals of 2,2'-bi-2-imidazolinium fumarate (**BI**/H^+)$_2$ (**FA**$^{-2}$) • 4H_2O grown from DMSO. (a) View of part of an alternating hydrogen-bonded tape composed of paired 2,2'-bi-2-imidazolinium monocations (**BI**/H^+) and fumarate dianions (**FA**$^{-2}$). Atoms of carbon are shown in gray, hydrogen in white, nitrogen in blue, and

oxygen in red. Hydrogen bonds are represented by broken lines. (b) View along the tapes, showing how they pack to form corrugated sheets and how the sheets stack to form the observed structure. Biimidazolinium monocations are shown in blue, fumarate dianions in red, and water molecules in white.

Detailed analysis of the structural parameters revealed interesting features. In particular, the biimidazolinium monocations are paired by cyclic hydrogen-bonded $\mathbf{R_2^2(10)}$ motifs closely similar to those observed in the structure of bis(amidine) **BI** itself, where the molecules are linked to form extended tapes.[31] In the fumarate salt, the N···H-N hydrogen bonds that link the biimidazolinium monocations have average N···N distances of 2.836 Å. Despite the potential for electrostatic repulsion between the paired cations, the observed distances are shorter than those in the structure of bis(amidine) **BI** (2.918 Å),[31] possibly because the monoprotonated form becomes a stronger acid. Monocations and dianions in the fumarate salt are connected by N-H···O hydrogen bonds with average N···O distances of 2.733 Å and average N-H···O angles of 151°. As expected, these structural parameters are similar to those observed in the corresponding oxalate salt, and they again confirm that hydrogen bonding is reinforced by electrostatic effects. The N-H···O bond distances in the fumarate salt are slightly longer than those in the oxalate salt, possibly because the bis(amidine) is only monoprotonated and because fumarate engages in additional hydrogen bonding to water. The various O···H-O hydrogen bonds that interconnect the tapes and sheets have average O···O distances in a normal range (2.760-2.829 Å). The solid-state ^{1}H NMR spectrum of the crystalline salt is

consistent with the observed structure, and its detailed interpretation is the subject of ongoing studies.

2,2'-Bi-2-imidazolinium terephthalate ($\mathbf{BI/H^+)_2}$ ($\mathbf{TA^{-2}}$). Mixing equimolar amounts of bis(amidine) **BI** and terephthalic acid (**TA**/H_2) in DMSO yielded crystals composed of a 2:1 ratio of biimidazolinium monocation **BI**/H^+ and terephthalate dianion ($\mathbf{TA^{-2}}$). Structural studies (see Table 1 for crystallographic parameters) confirmed the expected presence of tapes held together by charge-assisted hydrogen bonds. Again, however, double protonation of bis(amidine) **BI** did not occur, presumably because terephthalic acid has an even higher pK_a than oxalic and fumaric acids. Instead, the tapes were found to consist of an alternating arrangement of carboxylate dianions and dimers of the biimidazolinium monocation, as observed in the fumarate salt (Figure 5).

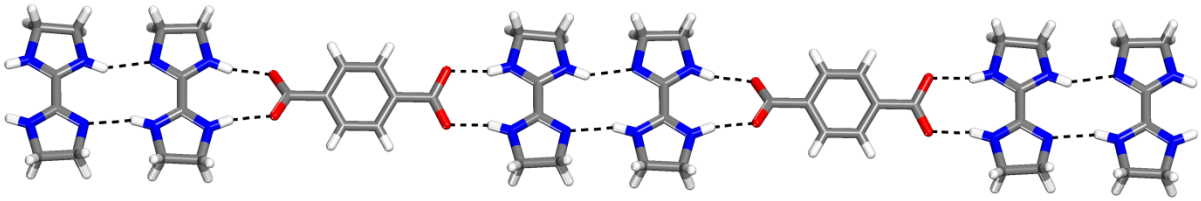

a

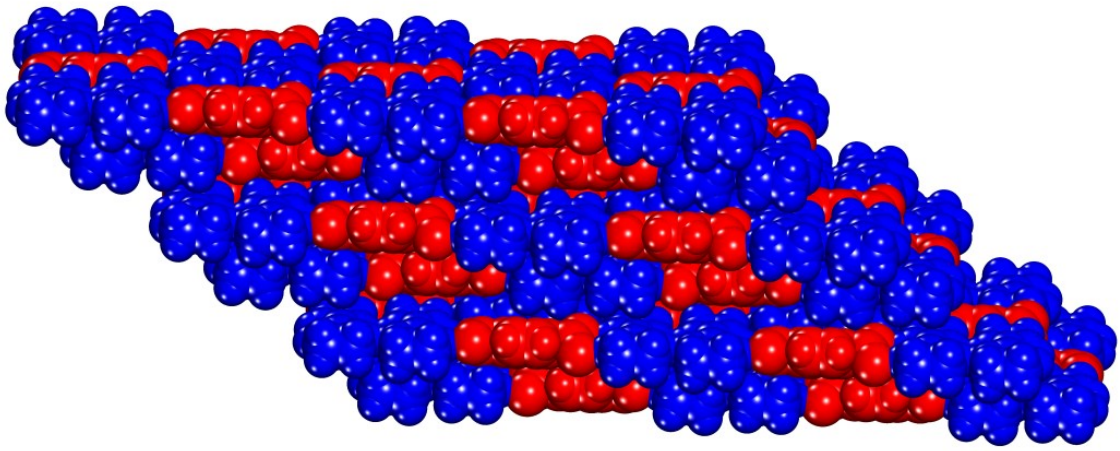

b

Figure 5. Representations of the structure of crystals of 2,2'-bi-2-imidazolinium terephthalate (**BI**/H^+)$_2$ (**TA**$^{-2}$) grown from DMSO. (a) View of part of an alternating hydrogen-bonded tape composed of paired 2,2'-bi-2-imidazolinium monocations (**BI**/H^+) and terephthalate dianions (**TA**$^{-2}$). Atoms of carbon are shown in gray, hydrogen in white, nitrogen in blue, and oxygen in red. Hydrogen bonds are shown as broken lines. (b) Side view of the tapes, showing how they pack to form sheets and how the sheets stack to form the observed structure. Biimidazolinium monocations are shown in blue and terephthalate dianions in red.

The biimidazolinium monocations are paired by the cyclic hydrogen-bonded $\mathbf{R_2^2(10)}$ motif observed in the structures of the fumarate salt and bis(amidine) **BI** itself.[31] The N···H-N hydrogen bonds linking the monocations have average N···N distances of 2.841 Å, which are again shorter than those in the structure of bis(amidine) **BI** (2.918 Å).[31] The monocations and dianions are connected by N-H···O hydrogen bonds with average N···O distances of 2.668 Å and average N-H···O angles of 164°. These parameters closely resemble those observed in the corresponding oxalate and fumarate salts, showing again that hydrogen bonding is reinforced by electrostatic effects. As in the case of the fumarate salt, the solid-state ^{1}H NMR spectrum of the terephthalate salt is consistent with the observed structure.

2,2'-Bi-2-imidazolinium trimesate ($\mathbf{BI/H^+)_2}$ ($\mathbf{TMA/H^{-2}}$) • $\mathbf{H_2O}$. Mixing bis(amidine) **BI** and trimesic acid (**TMA**/H_3) in a 3:2 molar ratio in DMSO yielded crystals that proved to be a monohydrated form of a 2:1 salt of biimidazolinium monocation **BI**/H^+ and trimesate dianion (**TMA**/H^{-2}). Crystallographic parameters are summarized in Table 1. The observed structure has features similar to those encountered in the corresponding fumarate and terephthalate salts. In particular, the biimidazolinium monocation is present, again presumably because the acid is not strong enough to effect double protonation. The resulting structure can be considered to consist of tapes with an alternating arrangement of carboxylate dianions and dimers of the biimidazolinium monocation (Figure 6). One of the carboxylate groups accepts two hydrogen bonds to form the standard $\mathbf{R_2^2(9)}$ motif observed in the oxalate, fumarate, and terephthalate salts, but the other adopts a bifurcated $\mathbf{R_2^1(7)}$ motif in which a single atom of oxygen serves as

acceptor. Inter-tape hydrogen bonding involving the remaining COOH group of the trimesate dianion and water joins the tapes into sheets.

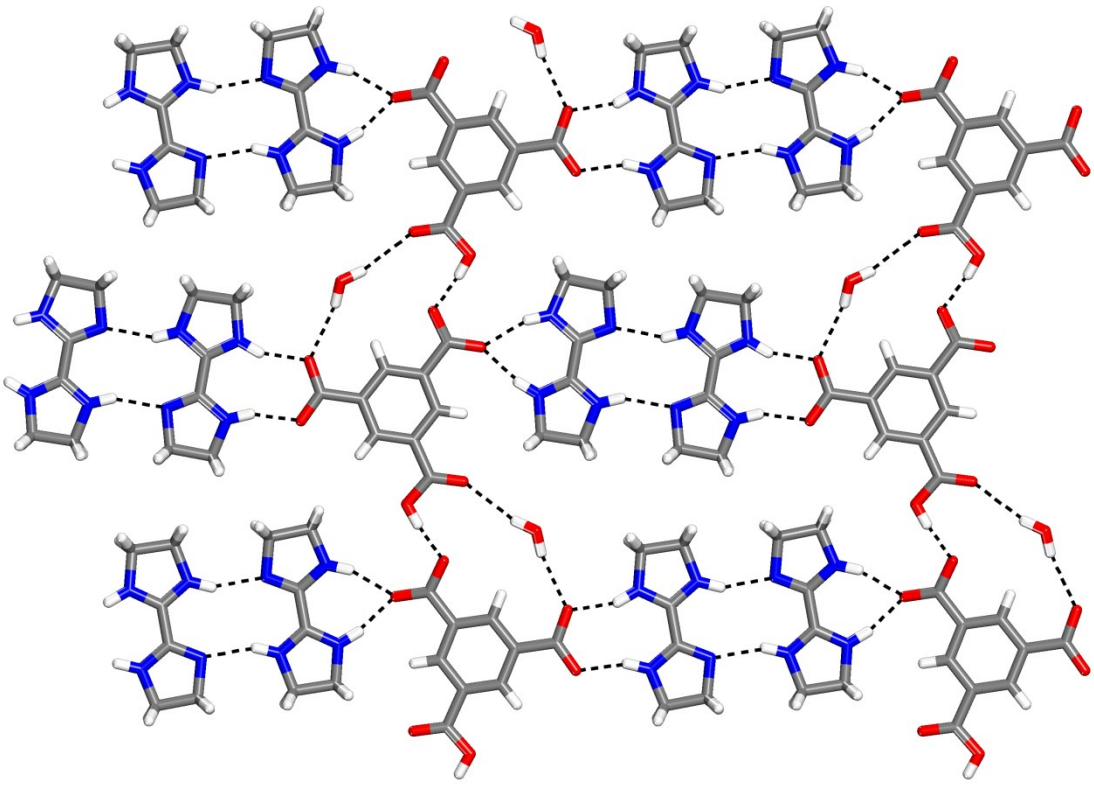

Figure 6. Representation of the structure of crystals of 2,2'-bi-2-imidazolinium trimesate (**BI**/H^+)$_2$ (**TMA**/H^{-2}) • H_2O grown from DMSO. View of part of a hydrogen-bonded sheet composed of paired 2,2'-bi-2-imidazolinium monocations (**BI**/H^+) and trimesate dianions (**TMA**/H^{-2}). Atoms of carbon are shown in gray, hydrogen in white, nitrogen in blue, and oxygen in red. Hydrogen bonds are shown as broken lines.

The geometric parameters closely match expectations based on the behavior of the corresponding fumarate and terephthalate salts. In particular, the N···H-N hydrogen bonds that link the biimidazolinium monocations into pairs have average N···N distances of 2.851 Å, and the N-H···O hydrogen bonds that link the monocations and carboxylate groups in $\mathbf{R_2^2(9)}$ motifs have average N···O distances of 2.695 Å and average N-H···O angles of 157°. The N-H···O hydrogen bonds in the bifurcated motif are longer (average N···O distance = 2.780 Å), as observed in related structures.[29-30] Strong O-H···O hydrogen bonds produced by the interaction COO^-···HOOC link the tapes into sheets (O···O distance = 2.478 Å). As in the case of the fumarate and terephthalate salts, the solid-state ^1H NMR spectrum of the trimesate salt is consistent with the observed structure.

2.5 Conclusions

As expected, protonation of cyclic bis(amidine) **BI** by oxalic, fumaric, terephthalic, and trimesic acids produces salts that crystallize to form structures with multiple charge-assisted hydrogen bonds corresponding to graph set $\mathbf{R_2^2(9)}$. In all cases, the geometry of the hydrogen-bonding sites programs the formation of tapes, which pack to form stacked sheets. The nature of the tapes depends on the pK_a of the acid used. Oxalic acid, the strongest of the series, effects double protonation of bis(amidine) **BI**, leading to the formation of tapes with alternating biimidazolinium dications and oxalate dianions interconnected by characteristic $\mathbf{R_2^2(9)}$ motifs that incorporate two charge-assisted N-H···O hydrogen bonds in nine-membered rings. The other acids monoprotonate bis(amidine) **BI**, producing similar alternating hydrogen-bonded tapes composed of paired biimidazolinium monocations and dicarboxylate dianions. In all cases, the observed N···O distances are shorter than those formed by neutral analogues, providing evidence that hydrogen bonding is strengthened by charge assistance.

The reliable formation of robust tapes and sheets in the 3D structures of carboxylate salts of bis(amidine) **BI** suggests that substances of this type are attractive candidates for producing predictably ordered 2D patterns of adsorption on suitable surfaces.[35-36] An additional opportunity for future exploration lies in studying salts of bis(amidine) **BI** and its analogues with acids that are strong enough to ensure diprotonation, such as complex sulfonic and phosphonic acids with multiple SO_2OH and $PO(OH)_2$ groups. Such studies are likely to

provide a deeper understanding of how charge-assisted hydrogen bonding can be used to direct molecular organization.

2.6 Experimental Section

General Notes. 2,2'-Bi-2-imidazoline (**BI**) was prepared by a published method.[22] Other compounds were purchased from commercial sources and used without further purification.

Syntheses and Characterizations of Salts

2,2'-Bi-2-imidazoline (**BI**) was mixed with the selected carboxylic acid in a 1:1 ratio (oxalic, fumaric, and terephthalic acids) or in a 3:2 ratio (trimesic acid), the solids were ground together, a small volume of DMSO was added, and the resulting mixture was heated briefly until the solids had dissolved. The resulting solution was then held at 25 °C to allow crystallization to occur.

2,2'-Bi-2-imidazolinium oxalate (BI/H_2^{+2}) (OA^{-2}). Isolated in 57% yield as colorless air-stable crystals: mp > 200 °C (dec); FTIR (ATR) 1276, 1299, 1579, 2400 (br) cm^{-1}; ^1H NMR (700 MHz, D_2O) δ 3.90 (s, 8H); ^{13}C NMR (175 MHz, D_2O) δ 46.1, 153.0, 170.5; ^1H solid-state NMR (600 MHz) δ 4.64 (s, 8H), 15.29 (s, 4H); HRMS (+ESI) calcd. for $C_6H_{11}N_4^+$ *m/e* 139.09837, found 139.09782. Anal. Calcd for $C_8H_{12}N_4O_4$: C, 42.11; H, 5.30. Found: C, 41.94; H, 5.51.

2,2'-Bi-2-imidazolinium fumarate $(BI/H^+)_2$ (FA^{-2}) • $4H_2O$. Isolated in 32% yield as colorless air-stable crystals: mp > 200 °C (dec); FTIR (ATR) 1282, 1372, 1569, 1685, 2600 (br) cm^{-1}; ^1H NMR (700 MHz, D_2O) δ 3.77 (s, 16H), 6.37 (s, 2H); ^{13}C NMR (175 MHz, D_2O) δ 39.0, 135.2, 161.3, 174.6; HRMS (+ESI) calcd. for $C_6H_{11}N_4^+$ *m/e* 139.09837, found 139.09589. Anal. Calcd for $C_{16}H_{24}N_8O_4 \bullet 3H_2O$: C, 43.04; H, 6.77. Found: C, 43.75; H, 6.52.

2,2'-Bi-2-imidazolinium terephthalate $(BI/H^+)_2$ (TA^{-2}). Isolated in 42% yield as colorless air-stable crystals: mp > 200 °C (dec); FTIR (ATR) 1376, 1496, 1682, 2500 (br) cm^{-1}; ^1H NMR (700 MHz, D_2O) δ 3.73 (s, 16H), 7.71 (s, 4H); ^{13}C NMR (175 MHz, D_2O) δ 47.1, 128.5, 138.5, 155.1, 175.1; HRMS (+ESI) calcd. for $C_6H_{11}N_4^+$ *m/e* 139.09837, found 139.09643. Anal. Calcd for $C_{20}H_{26}N_8O_4$: C, 54.29; H, 5.92; N, 25.32. Found: C, 53.91; H, 5.87; N, 24.93.

2,2'-Bi-2-imidazolinium trimesate $(BI/H^+)_2$ (TMA/H^{-2}) • H_2O. Isolated in 33% yield as colorless crystals: mp > 200 °C (dec); FTIR (ATR) 1281, 1360, 1570, 2800 (br) cm^{-1}; ^1H NMR (700 MHz, D_2O) δ 3.73 (s, 16H), 8.26 (s, 3H); ^{13}C NMR (175 MHz, D_2O) δ 47.0, 131.6, 136.2, 154.9, 174.2; HRMS (+ESI) calcd. for $C_6H_{11}N_4^+$ *m/e* 139.09837, found 139.09669. Anal. Calcd for $C_{21}H_{26}N_8O_6 \bullet H_2O$: C, 50.00; H, 5.59. Found: C, 50.20; H, 5.63.

X-Ray Crystallography

Structural analyses of single crystals were carried out with a Bruker AXS X8/Proteum Microstar diffractometer, using Cu Kα radiation produced by an FR591 rotating-anode generator equipped with multilayer HELIOS optics. Determinations of unit-cell lattices and collections of data were performed with the *APEX2* suite of software, data were integrated using *SAINT* software,[37] and a multi-scan absorption correction was applied using *SADABS*.[38] The structure were solved with SHELXS-97 and refined with SHELXL-97.[39] All non-hydrogen atoms were refined with anisotropic thermal displacement parameters. Hydrogen atoms were first located from the calculated difference-Fourier maps, then refined as riding atoms using the standard models from SHELXL-97. In the terephthalate salt (**BI**/H^+)$_2$ (**TA**$^{-2}$), one hydrogen atom of the **BI**/H^+ monocation is statistically disordered over two positions that are related by a twofold axis and have an equal occupancy factor of 0.5. For the trimesate salt (**BI**/H^+)$_2$ (**TMA**/H^{-2}) • H_2O, the included water was found to be disordered over two positions (O7A and O7B) with refined occupancy factors close to 0.5 (0.53/0.47).

Assessments of the homogeneity of bulk crystalline samples were carried out by comparing calculated diffraction patterns (generated using Mercury software)[40] with experimental patterns measured on a Bruker D8 Discover diffractometer with copper radiation (CuKα, λ = 1.5418 Å). The calculated and experimental patterns were closely similar, although small amounts of the acid used to form the salts were typically present in crystalline form as impurities.[41]

Acknowledgments. We are grateful to the Natural Sciences and Engineering Research Council of Canada, the Ministère de l'Éducation du Québec, the Canada Foundation for Innovation, the Canada Research Chairs Program, and Université de Montréal for financial support.

Supporting Information Available. Additional crystallographic details (tables of structural data in CIF format, thermal atomic displacement ellipsoid plots, and comparisons of calculated and experimental powder diffraction patterns). This information is available free of charge via the Internet at http://pubs.acs.org/.

2.7 Notes and References

1. Dunitz, J. D. *Chem. Commun.* **2003**, 545-548.
2. Desiraju, G. R. *Nature Mater.* **2002**, *1*, 77-79.
3. Gavezzotti, A. *Acc. Chem. Res.* **1994**, *27*, 309-314.
4. Maddox, J. *Nature* **1988**, *335*, 201.
5. Wuest, J. D. *Chem. Commun.* **2005**, 5830-5837.
6. Hosseini, M. W. *Acc. Chem. Res.* **2005**, *38*, 313-323.
7. Desiraju, G. R. *Acc. Chem. Res.* **2002**, *35*, 565-573.
8. Gilli, G.; Gilli, P. *The Nature of the Hydrogen Bond. Outline of a Comprehensive Hydrogen Bond Theory*; Oxford University Press: Oxford, 2009.
9. Ward, M. D. *Struct. Bonding (Berlin)* **2009**, *132*, 1-23.
10. Bernstein, J.; Davis, R. E.; Shimoni, L.; Chang, N.-L. *Angew. Chem., Int. Ed.* **1995**, *34*, 1555-1573.
11. Hosseini, M. W. *Coord. Chem. Rev.* **2003**, *240*, 157-166.
12. Stokes, F. A.; Coles, M. P.; Hitchcock, P. B. *CrystEngComm* **2012**, *14*, 771-773.
13. Han, J.; Zang, S.-Q.; Mak, T. C. W. *Chem. Eur. J.* **2010**, *16*, 5078-5088.
14. Yashima, E.; Maeda, K.; Iida, H.; Furusho, Y.; Nagai, K. *Chem. Rev.* **2009**, *109*, 6102-6211.
15. Reece, S. Y.; Nocera, D. G. *Annu. Rev. Biochem.* **2009**, *78*, 673-699.
16. Ferretti, V.; Bertolasi, V.; Pretto, L. *New J. Chem*. **2004**, 28, 646-651.

17. Corbellini, F.; Di Costanzo, L.; Crego-Calama, M.; Geremia, S.; Reinhoudt, D. N. *J. Am. Chem. Soc.* **2003**, *125*, 9946-9947.

18. Yang, J.; Melendez, R.; Geib, S. J.; Hamilton, A. D. *Struct. Chem.* **1999**, *10*, 221-228.

19. Terfort, A.; von Kiedrowski, G. *Angew. Chem., Int. Ed.* **1992**, *31*, 654-656.

20. Krechl, J.; Smrčková, S.; Pavlíková, F.; Kuthan, J. *Coll. Czech. Chem. Commun.* **1989**, *54*, 2415-2424.

21. Kraft, A. *J. Chem. Soc., Perkin Trans. 1* **1999**, 705-714.

22. Wang, J. C.; Bauman, J. E., Jr. *Inorg. Chem.* **1965**, *4*, 1613-1615.

23. For references, see: Stilinović, V.; Kaitner, B. *Cryst. Growth Des.* **2012**, *12*, 5763-5772.

24. Annamalai, V. R.; Linton, E. C.; Kozlowski, M. C. *Org. Lett.* **2009**, *11*, 621-624.

25. Piskov, V. B.; Kasperovich, V. P. *Zh. Org. Khim.* **1978**, *14*, 820-834.

26. Elguero, J.; Gonzalez, É.; Imbach, J.-L.; Jacquier, R. *Bull. Soc. Chim. Fr.* **1969**, 4075-4077.

27. Serjeant, E. P.; Dempsey, B. *Ionization Constants of Organic Acids in Aqueous Solution*; Pergamon: Oxford, 1979.

28. Braude, E. A; Nachod, F. C. *Determination of Organic Structures by Physical Methods*; Academic Press: New York, 1955.

29. Taylor, R.; Kennard, O. *Acc. Chem. Res.* **1984**, *17*, 320-326.

30. Taylor, R.; Kennard, O.; Versichel, W. *Acta. Crystallogr.* **1984**, *B40*, 280-288.

31. Brennan, C. J.; McKee, V. *Acta Crystallogr.* **1999**, *C55*, 1492-1494.

32. Caltagirone, C.; Hiscock, J. R.; Hursthouse, M. B.; Light, M. E.; Gale, P. A. *Chem. Eur. J.* **2008**, *14*, 10236-10243.

33. Cao, M.; Hu, B.; Luo, F.; Cheng, C.; Hu, Z. *Acta Crystallogr.* **2007**, *E63*, m2927.

34. Martinez Lorente, M. A.; Dahan, F.; Sanakis, Y.; Petrouleas, V.; Bousseksou, A.; Tuchagues, J.-P. *Inorg. Chem.* **1995**, *34*, 5346-5357.

35. Duong, A.; Dubois, M.-A.; Maris, T.; Métivaud, V.; Yi, J.-H.; Nanci, A.; Rochefort, A.; Wuest, J. D. *J. Phys. Chem. C* **2011**, *115*, 12908-12919.

36. Duong, A.; Maris, T.; Wuest, J. D. *CrystEngComm* **2011**, *13*, 5571-5577.

37. *APEX2* and *SAINT*, *Version 7.68A*; Bruker AXS Inc.: Madison, WI 53719-1173, 2009.

38. Sheldrick, G. M., *SADABS*, *Version 2008/1*; Bruker AXS Inc.: Madison, WI 53719-1173, 2008.

39. Sheldrick, G. M. *Acta Crystallogr*. **2008**, *A64*, 112-122.

40. Macrae, C. F.; Bruno, I. J.; Chisholm, J. A.; Edgington, P. R.; McCabe, P.; Pidcock, E.; Rodriguez-Monge, L.; Taylor, R.; van de Streek, J.; Wood, P. A. *J. Appl. Cryst*. **2008**, *41*, 466-470.

41. For details, see the Supporting Information.

For Table of Contents Use Only

Table of Contents Graphic

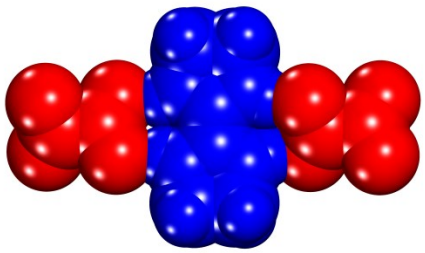

Table of Contents Synopsis

2,2'-Bi-2-imidazoline, a cyclic bis(amidine), reacts with oxalic, fumaric, terephthalic, and trimesic acids, producing salts that crystallize to form networks with features resulting predictably from the geometry of the ions and their ability to engage in multiple charge-assisted hydrogen bonds according to reliable motifs.

2.8 Conclusion

Chapter 2 describes molecular networks created by the association of four different carboxylate anions with cations derived from 2,2'-bi-2-imidazoline. The resulting structures were found to incorporate multiple charge-assisted hydrogen bonds between the ionic components. The geometry and pK_a values of the carboxylic acids used were among the factors that helped determine the nature of the structures. In all cases studied, the geometry of the components and of the preferred hydrogen-bonding motifs led to the formation of tapes, which then packed to form stacked sheets. The large differences in pK_a values between protonated forms of 2,2'-bi-2-imidazoline and typical carboxylic acids led reliably to proton transfer from the acids to the bis(amidine). The pK_a value of the acid involved determined the extent of proton transfer, and it was only in the case of the strongest acid used (oxalic acid) that diprotonation of the bis(amidine) occurred, leading to the formation of a different type of tape. The present work sets the stage for future studies using acids with lower pK_a values and more complex geometries. For instance, acids that are strong enough to ensure the diprotonation of 2,2'-bi-2-imidazoline, such as phosphonic acids with multiple $PO(OH)_2$ groups, are candidates of special interest. Those acids were chosen for an extension of the study, and the results are discussed in detail in Chapter 3.

2.9 Contribution of Co-Authors

The principal author performed the synthesis and characterization of the compounds presented in this article, and she obtained them in crystalline form. In addition, she wrote the corresponding parts of the first draft of the manuscript that has been published and forms the body of Chapter 2. Thierry Maris determined the structure of the crystals by X-ray diffraction, and he also contributed to the manuscript by preparing illustrations and by proof-reading initial drafts. Cédric Malveau contributed by obtaining solid-state NMR spectra of the crystals. Daniel Beaudoin and Fatima Helzy provided several key ideas underlying the design of the project. James D. Wuest supervised the research and contributed to writing the manuscript.

3.0 Chapter 3 : Article 3

Lie, S.; Maris, T.; Wuest, J. D.

" Molecular Networks Created by Charge-Assisted Hydrogen Bonding in Phosphonate, Phosphate, and Sulfonate Salts of Bis(amidines)" *Cryst. Growth Des.* Submitted for publication.

3.1 Introduction

Chapter 3, presented in the form of a manuscript which has been submitted for publication in *Cryst. Growth Des*., summarizes how 2,2'-bi-2-imidazoline and a related bis(amidine), fluoflavin, are protonated by various phosphonic and sulfonic acids and how the resulting ions are arranged in crystalline salts. The salts were found to consist of extended ionic networks in which the components are held together by multiple charge-assisted hydrogen bonds. As planned, phosphonic acids have higher acidities than carboxylic acids and can therefore diprotonate 2,2'-bi-2-imidazoline, whereas fluoflavin is less basic and was observed to be doubly protonated only by stronger acids such as phosphoric acid. Although charge-assisted N-H···O hydrogen bonds were observed to play a key role in directing association, additional O-H···O hydrogen bonds were formed between phosphonate anions, leading to the formation of more extensively bonded networks.

Molecular Networks

Created by Charge-Assisted Hydrogen Bonding

in Phosphonate, Phosphate, and Sulfonate Salts of Bis(amidines)

Sharon Lie, Thierry Maris, and James D. Wuest*

Département de Chimie, Université de Montréal, Montréal, Québec H3C 3J7

Canada

Abstract

Two bis(amidines), 2,2'-bi-2-imidazoline (**BI**) and fluoflavin (**FF**), were treated with phosphonic, phosphoric, and sulfonic acids in an effort to produce crystalline salts composed of ions linked by networks of charge-assisted hydrogen bonds. As intended, mixing bis(amidine) **BI** with 1,4-benzenediphosphonic acid and 1,3,5-benzenetriphosphonic acid yielded crystals of phosphonate salts of dication $H_2\mathbf{BI}^{+2}$. Structural analyses showed that such salts tend to incorporate tapes composed of alternating dications and anions linked by multiple charge-assisted N-H···O hydrogen bonds of type $\mathbf{R_2^2(9)}$ and $\mathbf{R_2^1(7)}$. Typically, the tapes are further connected to form sheets or other assemblies by additional O-H···O hydrogen bonds involving phosphonate anions. An analogous reaction of the more weakly basic bis(amidine) **FF** with 1,4-benzenedisulfonic acid yielded only a sulfonate salt of monocation $H\mathbf{FF}^{+}$; however, diprotonation could be achieved by phosphoric acid to produce a crystalline salt built from stacks of $H_2\mathbf{FF}^{+2}$ dications linked to phosphate anions by charge-assisted N-H···O hydrogen bonds of type $\mathbf{R_2^2(8)}$. Together, these results demonstrate that acids with multiple $PO(OH)_2$ and SO_2OH groups can react with bis(amidines) to produce salts with structural features resulting predictably from the geometry of the ions and their ability to engage in multiple charge-assisted hydrogen bonds according to standard patterns.

Introduction

Molecular organization in materials reflects the topology of the individual components and the combined effects of diverse intermolecular interactions. When the structures are well defined, when particular interactions are dominant, and when these factors work in synergy to control how neighboring molecules are positioned, overall organization can often be predicted with confidence.[1-2] Among interactions most suitable for controlling organization in this way are hydrogen bonds, which offer high directionality and strength, particularly when reinforced by electrostatic attraction between species of opposite charge.[3]

In recent work,[4] we have shown that such charge-assisted hydrogen bonding can be used to control molecular organization in crystals of carboxylate salts derived from 2,2'-bi-2-imidazoline (**BI**),[5] a bis(amidine). Dicarboxylic acids strong enough to convert bis(amidine) **BI** into dication

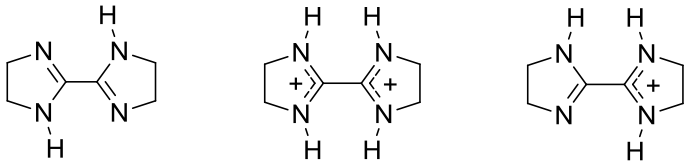

H_2**BI**$^{+2}$ by double protonation were found to yield structures built from tapes of alternating dicarboxylate dianions and bis(amidinium) dications, linked by cyclic arrays of charge-assisted hydrogen bonds (Figure 1a). These arrays can be described by the graph set $\mathbf{R_2^2(9)}$, where **R** denotes a cyclic motif, the superscript and subscript give the number of hydrogen-bond acceptors and donors, respectively, and the size of the ring is indicated in parentheses.[6]

Adjacent tapes pack closely to form sheets, which then stack to form the observed three-dimensional structures. In contrast, weaker dicarboxylic acids produce only monocation H**BI**$^{+}$ and favor a second family of tapes (Figure 1b), in which hydrogen-bonded dimers of the monocation are connected to dicarboxylate dianions by charge-assisted hydrogen bonds of type $\mathbf{R_2^2(9)}$. For example, oxalic acid (pK_{a1} 1.23) effects double protonation of bis(amidine) **BI**, and the resulting salt crystallizes according to the motif shown in Figure 1a. However, weaker dicarboxylic acids such as fumaric acid (pK_{a1} 3.02) and terephthalic acid (pK_{a1} 3.51) only monoprotonate the bis(amidine), and their salts have structures of the type shown in Figure 1b. As a result, efforts to engineer crystals derived from bis(amidine) **BI** and compounds with multiple COOH groups must take values of pK_a into account.

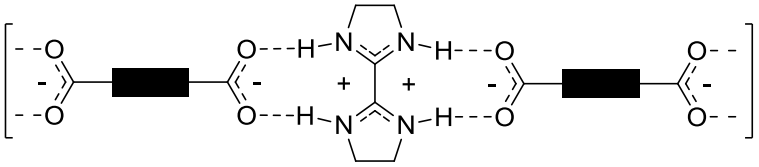

a

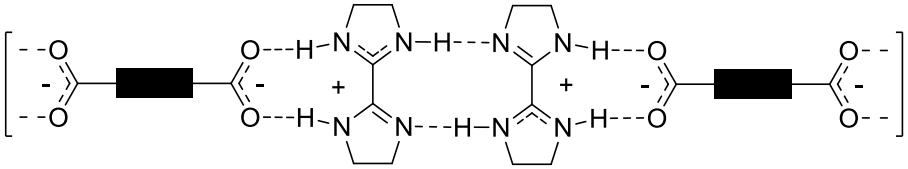

b

Figure 1. Representation of tapes linked by charge-assisted hydrogen bonds according to the graph set $\mathbf{R_2^2(9)}$, formed by the interaction of dicarboxylate dianions with (a) bis(amidinium) dication H$_2$**BI**$^{+2}$ and (b) the hydrogen-bonded dimer of monocation H**BI**$^{+}$.

To avoid this complication, we turned to salts prepared by treating bis(amidines) with phosphonic acids and sulfonic acids, which are much stronger than the corresponding carboxylic acids.[7-9] We reasoned that compounds with multiple $PO(OH)_2$ and SO_2OH groups would reliably diprotonate bis(amidine) **BI** and close analogues, thereby producing a single family of networks in which bis(amidinium) dications are linked to phosphonate and sulfonate anions by multiple charge-assisted hydrogen bonds. To test this possibility, we have made salts of two related bis(amidines), compound **BI** and fluoflavin (**FF**), with various complex phosphonic and sulfonic acids, including 1,4-benzenediphosphonic acid (H_4**BDP**), 1,3,5-benzenetriphosphonic acid (H_6**BTP**), and 1,4-benzenedisulfonic acid (H_2**BDS**). After significant effort, we crystallized several of these salts and simple analogues, and we now report their structures.

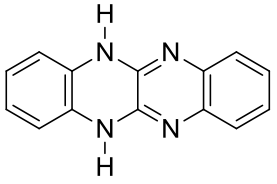

FF

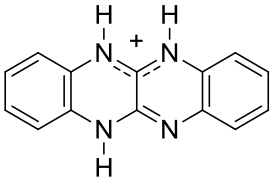

HFF^+

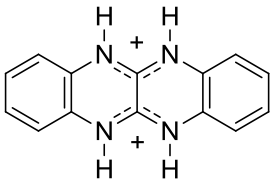

H_2FF^{+2}

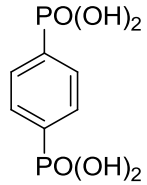

H_4**BDP**

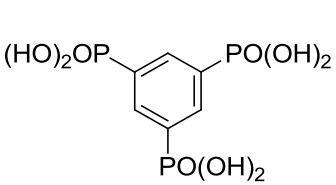

H_6**BTP**

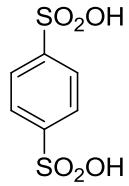

H_2**BDS**

Results and Discussion

2,2'-Bi-2-imidazoline (**BI**)[5] and fluoflavin (**FF**)[10] were prepared by known methods and mixed in specific ratios with phosphonic, phosphoric, and sulfonic acids. Ethyl esters of diphosphonic acid H_4**BDP** and triphosphonic acid H_6**BTP** were made by published methods[11] and converted into the corresponding acids by hydrolysis under standard conditions.[12,13] Disulfonic acid H_2**BDS** was made by a known procedure.[14] Both bis(amidines) **BI** and **FF** reacted with the various acids to give salts, due to the large differences in pK_a between those of typical amidinium cations (10-11)[15-18] and those of arylphosphonic and arylsulfonic acids.[7-9] Single crystals of salts were grown from various solvents, and their structures were resolved by X-ray diffraction to confirm the composition of the salts and to reveal the nature of the interionic interactions.

2,2'-Bi-2-imidazolinium 1,4-benzenediphosphonate (H_2BI**$^{+2}$) (H_2**BDP**$^{-2}$)**. Crystals were obtained by preparing separate solutions of bis(amidine) **BI** and 1,4-benzenediphosphonic acid (H_4**BDP**) in 3:2 EtOH/H_2O, mixing them in a 1:1 molar ratio, and allowing the combined solution to undergo slow evaporation at 25 °C. This procedure yielded crystals of two forms, one with the composition (**H_2BI**$^{+2}$) (H_2**BDP**$^{-2}$). Crystals of this form could also be grown from DMSO. Their structure was determined by X-ray diffraction, and crystallographic parameters are summarized in Table 1. Our structural analyses were consistent with expectations, including double protonation of bis(amidine) **BI** and the formation of tapes built from an alternating arrangement of bis(amidinium) dications (**H_2BI**$^{+2}$) and benzenediphosphonate dianions (H_2**BDP**$^{-2}$), interconnected by charge-assisted N–H···O hydrogen bonds (Figure 2). In

addition, each dianion forms O–H···O hydrogen bonds to two other dianions in adjacent tapes, thus leading to the formation of slightly corrugated sheets, which stack to form the observed structure (Figure 2).

Table 1. Crystallographic data for salts (H_2**BI**$^{+2}$) (H_2**BDP**$^{-2}$), (H_2**BI**$^{+2}$) (H_2**BDP**$^{-2}$) • 2DMSO, (H_2**BI**$^{+2}$) (H_2**BDP**$^{-2}$) • 4H_2O, and (H_2**BI**$^{+2}$) (H_4**BTP**$^{-2}$) • DMSO.

salt	(H_2**BI**$^{+2}$) (H_2**BDP**$^{-2}$)	(H_2**BI**$^{+2}$) (H_2**BDP**$^{-2}$) • 2DMSO	(H_2**BI**$^{+2}$) (H_2**BDP**$^{-2}$) • 4H_2O	(H_2**BI**$^{+2}$) (H_4**BTP**$^{-2}$) • DMSO
crystallization medium	DMSO	DMSO	EtOH/H_2O	DMSO
formula	$C_{12}H_{18}N_4O_6P_2$	$C_{16}H_{30}N_4O_8P_2S_2$	$C_{12}H_{26}N_4O_{10}P_2$	$C_{14}H_{25}N_4O_{10}P_3S$
crystal system	monoclinic	triclinic	monoclinic	triclinic
space group	$P2_1/n$	$P\bar{1}$	$P2_1/c$	$P\bar{1}$
a (Å)	9.0366(5)	4.8022(5)	10.1046(5)	7.513(2)
b (Å)	8.0286(4)	10.3715(10)	8.5162(5)	11.899(3)
c (Å)	10.8628(6)	12.1080(11)	11.6426(6)	12.077(3)
α (°)	90	99.771(5)	90	95.688(13)
β (°)	107.809(3)	93.061(6)	109.58(3)	94.235(14)
γ (°)	90	99.947(5)	90	94.317(13)
V (Å^3)	750.34(7)	583.24(10)	943.9(2)	1067.8(5)
Z	2	1	2	2
T (K)	100	150	100	150
ρ_{calc} (g cm^{-3})	1.665	1.516	1.577	1.662
μ (mm^{-1})	3.030	3.820	2.667	4.049
crystal size (mm)	0.08 × 0.07 × 0.04	0.08 × 0.08 × 0.04	0.15 × 0.11 × 0.10	0.18 × 0.11× 0.06
θ range (°)	5.59-70.95	3.72-68.05	4.64-70.82	3.69-69.72
measured reflections	25205	10321	6920	18830
independent reflections	1442	2109	1784	3458
R_1, $I > 2\sigma(I)$	0.0474	0.0796	0.0435	0.1244
R_1, all data	0.0519	0.0885	0.0507	0.1574
wR_2, $I > 2\sigma(I)$	0.1283	0.2157	0.1145	0.3369
wR_2, all data	0.1327	0.2222	0.1213	0.3599
GoF	1.065	1.097	1.040	1.290

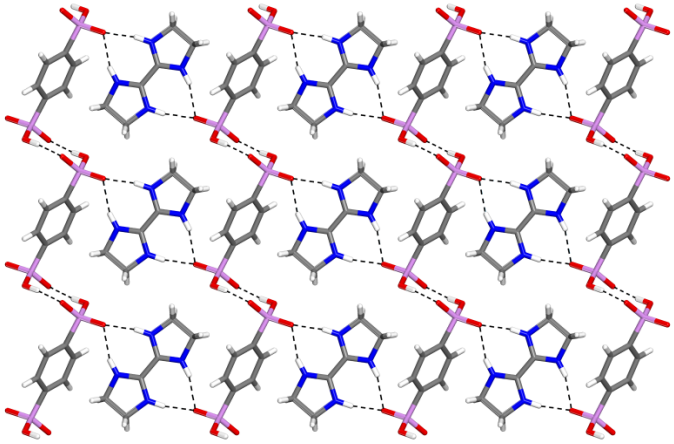

a

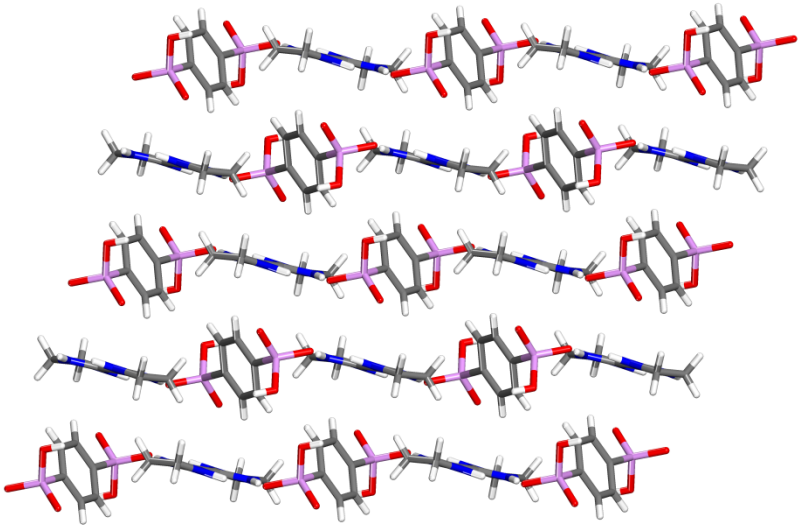

b

Figure 2. Representations of the structure of crystals of 2,2'-bi-2-imidazolinium 1,4-benzenediphosphonate (H_2**BI**$^{+2}$) (H_2**BDP**$^{-2}$) grown from DMSO or EtOH/H_2O. (a) View of part of three tapes composed of alternating bis(amidinium) dications (H_2**BI**$^{+2}$) and diphosphonate dianions (H_2**BDP**$^{-2}$), linked by charge-assisted N–H···O hydrogen bonds of

type $\mathbf{R_2^1(7)}$. The tapes are interconnected to form slightly corrugated sheets by O–H···O hydrogen bonding of phosphonate anions according to standard motif $\mathbf{R_2^2(8)}$. Hydrogen bonds are shown as broken lines. (b) Side view showing stacking of the sheets. In both images, atoms of carbon are shown in gray, hydrogen in white, nitrogen in blue, oxygen in red, and phosphorus in purple.

Detailed examination of the structure suggests that the bis(amidinium) dications and diphosphonate dianions are linked by seven-membered rings incorporating two charge-assisted N–H···O hydrogen bonds according to motif $\mathbf{R_2^1(7)}$. Related motifs have been reported previously.[19] Full transfer of two protons from the diphosphonic acid to the bis(amidine) is consistent with the observation of two nearly equal C-N bond lengths within each $\mathbf{R_2^1(7)}$ motif (1.306(3) and 1.308(3) Å). In this motif, a single anionic oxygen atom of each phosphonate moiety serves as a bifurcated acceptor of two hydrogen bonds. In contrast, cations derived from bis(amidine) **BI** have been shown to interact with analogous carboxylate anions by forming nine-membered rings incorporating charge-assisted N–H···O hydrogen bonds of alternative type $\mathbf{R_2^2(9)}$.[4] This difference in behavior can be attributed in large part to geometric factors, including the length of P-O bonds in phosphonates (which are longer than C-O bonds in carboxylates) and the size of O-P-O angles (which are smaller than O-C-O angles in carboxylates). Specifically, the lengths of the P-O^- bonds in phosphonate salt ($H_2\mathbf{BI}^{+2}$) ($H_2\mathbf{BDP}^{-2}$) are 1.5120(16) and 1.5099(17) Å, and the O-P-O angle is 115.97(10)°; in contrast, the average length of the corresponding C-O bonds in the oxalate salt is 1.2572(12) Å, and the average O-C-O angle is 125.80(15)°. Despite the preference of phosphonate salt ($H_2\mathbf{BI}^{+2}$) ($H_2\mathbf{BDP}^{-2}$) for the $\mathbf{R_2^1(7)}$ motif, however, metal-coordinated derivatives of

bis(amidine) **BI** and related compounds have been observed to engage in hydrogen bonds of type $\mathbf{R_2^2(9)}$ with phosphate anions, at least when N-C-C angles within the motif are opened by the effect of coordination.[20-21]

In bis(amidinium) phosphonate (H_2**BI**$^{+2}$) (H_2**BDP**$^{-2}$), N–H···O hydrogen bonds that link the dications and dianions into tapes have relatively short N···O distances (2.706 (2) and 2.850(3) Å), and the N–H···O bond angles have an average value of 165.0°. In the analogous oxalate salt, the N···O distance is slightly shorter (2.656 Å), presumably because hydrogen bonds to the acceptor are not bifurcated, and the N–H···O bond angle is 160.70°.[22] Both salts have N···O distances shorter than those normally observed in non-ionic cocrystals incorporating N···H-O interactions without full protonation of N (2.85 Å).[23-24] We conclude that the hydrogen bonds in phosphonate salt (H_2**BI**$^{+2}$) (H_2**BDP**$^{-2}$) are strengthened by charge assistance.

Adjacent tapes in the phosphonate salt are linked to form sheets by O–H···O hydrogen bonding characteristic of simple arylphosphonic acids and their monoanions (Figure 2a), which form chair-shaped pairs defined by cyclic motif $\mathbf{R_2^2(8)}$.[19,25-28] The O···O distance (2.595(2) Å) and O–H···O angle (173°) are normal. As a result, all ions in each sheet are interconnected by a two-dimensional network of hydrogen bonds; in contrast, hydrogen bonding in sheets of the corresponding oxalate is confined to one dimension, aligned with individual tapes. Sheets in the phosphonate salt stack to give the observed structure, with no noteworthy interactions between the sheets (Figure 2b).

2,2'-Bi-2-imidazolinium 1,4-benzenediphosphonate (H_2BI^{+2}**) (**H_2**BDP^{-2}**) • 2DMSO**. In addition to producing crystals of composition (H_2**BI**$^{+2}$) (H_2**BDP**$^{-2}$), mixing bis(amidine) **BI** and 1,4-benzenediphosphonic acid (H_4**BPD**) in a 1:1 ratio in DMSO also yielded crystals of composition (H_2**BI**$^{+2}$) (H_2**BDP**$^{-2}$) • 2DMSO. The structure of this second form was resolved, and crystallographic parameters are presented in Table 1. Analysis again suggested the full transfer of two protons from the diphosphonic acid to the bis(amidine) and revealed the expected presence of tapes built from alternating bis(amidinium) dications and diphosphonate dianions (Figure 3a), connected by charge-assisted N–H···O hydrogen bonds of type $\mathbf{R_2^1(7)}$. In these motifs, the N···O distances (2.669(5) and 2.757(5) Å) and average N-H···O angle (163°) have values that are normal for charge-assisted hydrogen bonds.

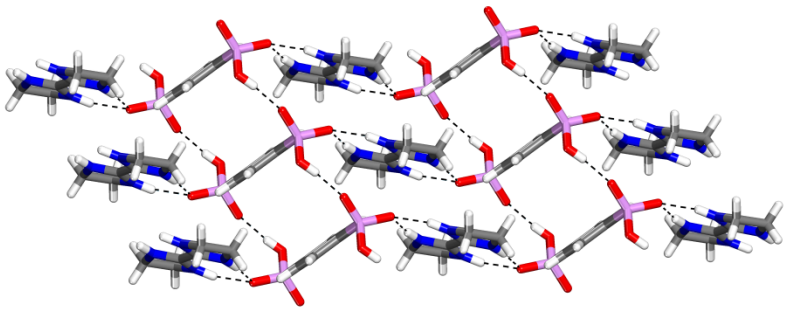

a

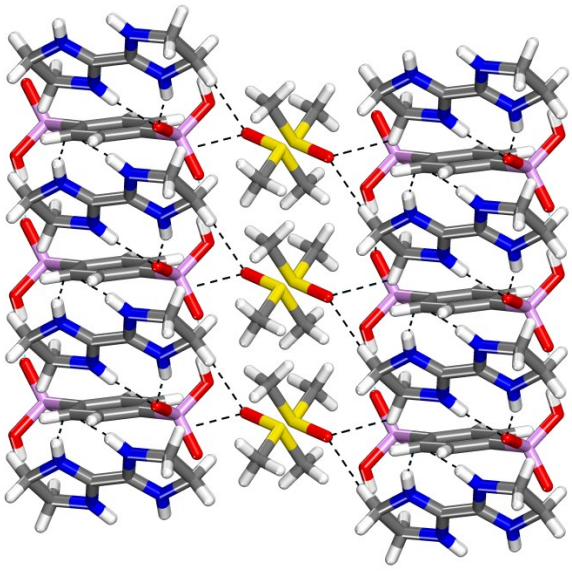

b

Figure 3. Representations of the structure of crystals of 2,2'-bi-2-imidazolinium 1,4-benzenediphosphonate (H_2**BI**$^{+2}$) (H_2**BDP**$^{-2}$) • 2DMSO grown from DMSO. (a) View of part of three tapes composed of alternating bis(amidinium) dications (H_2**BI**$^{+2}$) and diphosphonate dianions (H_2**BDP**$^{-2}$), linked by charge-assisted N–H···O hydrogen bonds of type $\mathbf{R_2^1(7)}$. The tapes are interconnected to form sheets by additional O–H···O hydrogen bonding of phosphonate anions. Hydrogen bonds are shown as broken lines. (b) Side view showing how the ionic sheets are separated by layers of included DMSO. In both images, atoms of carbon are shown in gray, hydrogen in white, nitrogen in blue, oxygen in red, phosphorus in purple, and sulfur in yellow.

The tapes lie along the *ab* diagonal and are connected to form sheets in the *ab* plane by O–H···O hydrogen bonding of phosphonate anions (Figure 3a), with normal O···O distances

(2.552(5) Å) and O–H···O angles (167°). These interactions create columns of diphosphonate dianions stacked within the sheets along the *a* axis. In the observed structure, the ionic sheets are separated by intervening layers of DMSO (Figure 3b).

We conclude that crystals of the salt (H_2**BI**$^{+2}$) (H_2**BDP**$^{-2}$), both as the DMSO solvate and the unsolvated form, incorporate closely similar tapes made up of alternating bis(amidinium) dications and diphosphonate dianions held together by charge-assisted N–H···O hydrogen bonds of type $\mathbf{R_2^1(7)}$. Appearance of the tapes in both structures suggests that they are a dominant associative motif.

2,2'-Bi-2-imidazolinium 1,4-benzenediphosphonate (H_2BI^{+2}) (H_2BDP^{-2}) • 4H_2O. In addition to producing unsolvated crystals of composition (H_2**BI**$^{+2}$) (H_2**BDP**$^{-2}$), mixing bis(amidine) **BI** and 1,4-benzenediphosphonic acid (H_4**BPD**) in a 1:1 ratio in 3:2 EtOH/H_2O also produced crystals of tetrahydrate (H_2**BI**$^{+2}$) (H_2**BDP**$^{-2}$) • 4H_2O. The structure of this additional form was resolved, and Table 1 summarizes various crystallographic parameters. Again, the data suggest that complete transfer of two protons from the diphosphonic acid to the bis(amidine) was achieved, and the resulting diphosphonate dianions and bis(amidinium) dications participate in the formation of an extensively hydrogen-bonded network. However, the dianions and dications are not linked directly to form normal tapes; instead, they interact indirectly through intervening molecules of H_2O (Figure 4).

Detailed analysis of the structure revealed chains of 1,4-benzenediphosphonate dianions linked end-to-end along the *b* axis by normal O–H···O hydrogen bonding of type $\mathbf{R_2^2(8)}$, as

shown in Figure 4a. The resulting hydrogen-bonded rings adopt chair conformations with normal O···O distances (2.598(2) Å) and O–H···O angles (166°). Each diphosphonate dianion forms additional hydrogen bonds with six molecules of H_2O, some of which serve to connect adjacent chains to form corrugated anionic sheets parallel to the *bc* plane. Each bis(amidinium) dication interacts with two molecules of H_2O to form $\mathbf{R_2^1(7)}$ motifs in which the atoms of oxygen act as acceptors of bifurcated N–H···O hydrogen bonds (Figure 4b), with normal N···O distances (2.773(3) and 2.786(3) Å) and average N-H···O angle (166(3)°). Each dihydrated dication is then linked by hydrogen bonds involving H_2O to six surrounding diphosphonate dianions. The overall structure can be described as being comprised of corrugated anionic hydrogen-bonded sheets of diphosphonate dianions, separated by layers of bis(amidinium) dications (Figure 4c).

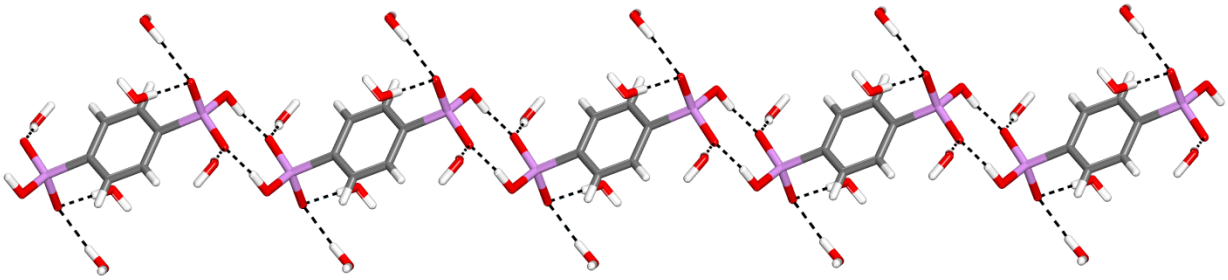

a

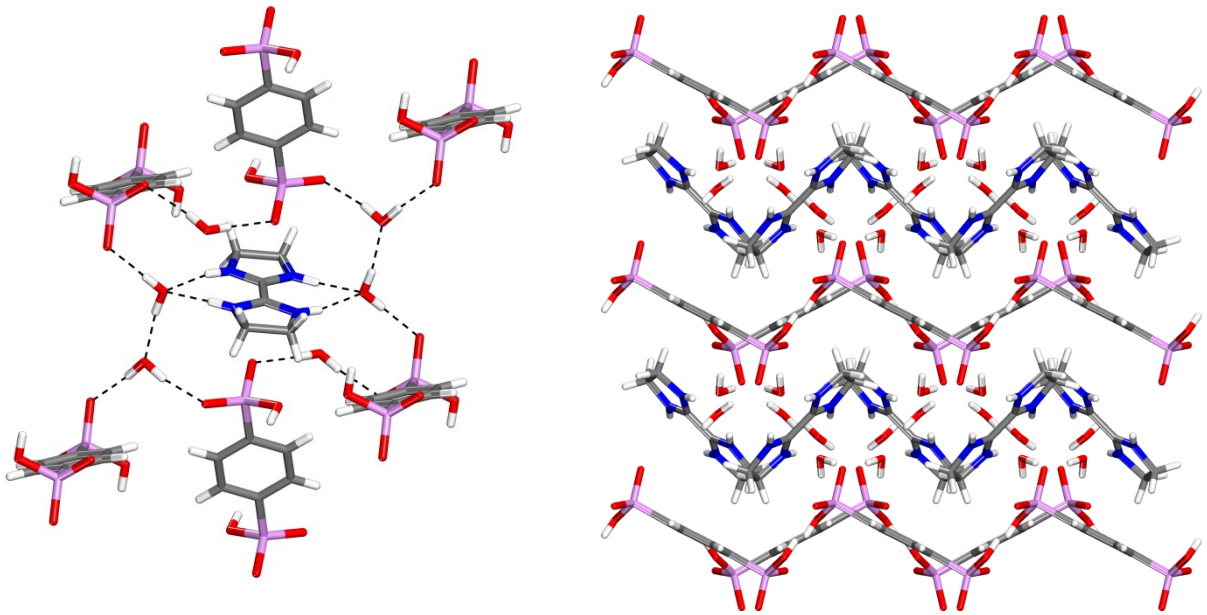

Figure 4. Representations of the structure of crystals of 2,2'-bi-2-imidazolinium 1,4-benzenediphosphonate (H_2**BI**$^{+2}$) (H_2**BDP**$^{-2}$) • 4H_2O grown from 3:2 EtOH/H_2O. (a) View of part of a hydrogen-bonded chain of 1,4-benzenediphosphonate dianions and associated molecules of H_2O. (b) View of a dihydrated bis(amidinium) dication and surrounding diphosphonate dianions, linked indirectly by hydrogen bonds to intervening molecules of H_2O. (c) Side view of corrugated anionic sheets of diphosphonate dianions and intervening layers of bis(amidinium) dications. Atoms of carbon are shown in gray, hydrogen in white, nitrogen in blue, oxygen in red, and phosphorus in purple. Hydrogen bonds are shown as broken lines.

2,2'-Bi-2-imidazolinium 1,3,5-benzenetriphosphonate (H_2BI**$^{+2}$) (H_4**BTP**$^{-2}$) • DMSO.** Crystals of the salt (H_2**BI**$^{+2}$) (H_4**BTP**$^{-2}$) • DMSO were obtained by mixing bis(amidine) **BI** and 1,3,5-benzenetriphosphonic acid (H_6**BTP**) in a 3:2 molar ratio in DMSO and by allowing the solution to stand at 25 °C. The structure was determined, and crystallographic parameters are summarized in Table 1. Analysis suggested that dication H_2**BI**$^{+2}$ was formed as expected by the transfer of two protons from triphosphonic acid H_6**BTP** to bis(amidine) **BI**. The structure incorporates parallel tapes built from an alternating arrangement of bis(amidinium) dications and triphosphonate dianions linked by charge-assisted N–H···O hydrogen bonds (Figure 5a). In the tapes, each dication is connected to the next by a single bridging phosphonate group, which engages in two distinct cyclic patterns of hydrogen bonding. One gives a nine-membered motif $\mathbf{R_2^2(9)}$, in which both O^- and OH of the phosphonate group serve as acceptors. In this motif, the N···O distances are 2.689(12) and 2.975(12) Å, and the corresponding N–H···O angles are 165 and 142°, respectively. In the second pattern of charge-assisted hydrogen bonding, a single O^- acts as acceptor to produce a standard bifurcated $\mathbf{R_2^1(7)}$ motif, as seen in other amidinium phosphonates derived from compound **BI**. In this second motif, the N···O distances are 2.660(11) and 2.768(11) Å, and the corresponding N–H···O angles are 163 and 159°, respectively.

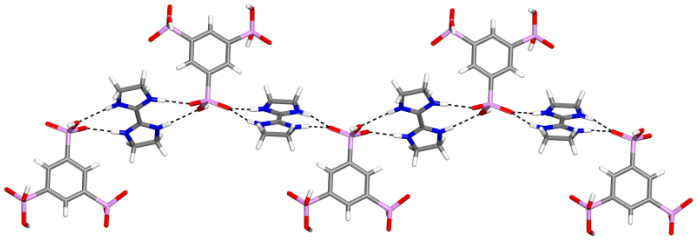

a

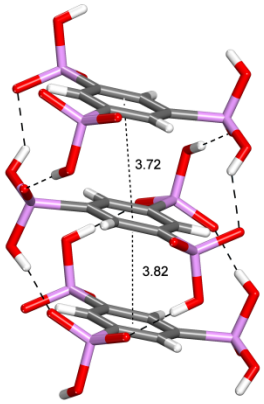

b

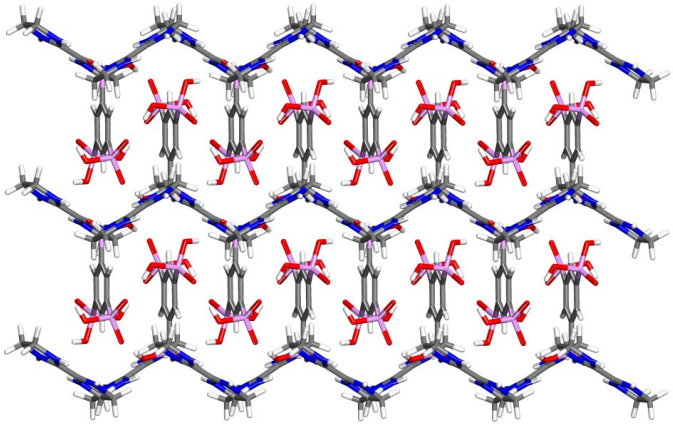

c

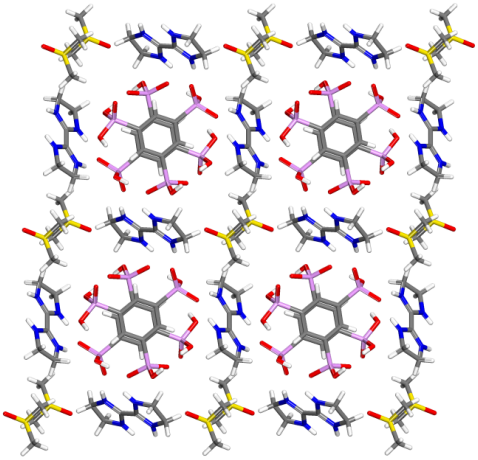

d

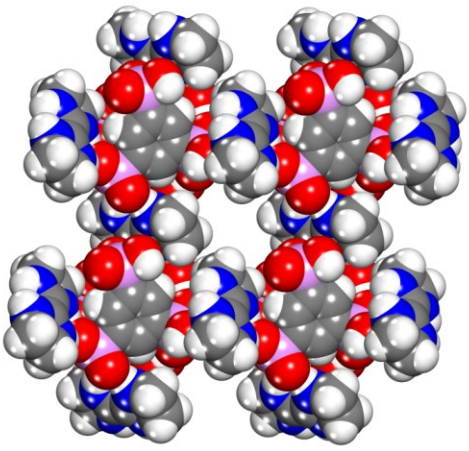

e

Figure 5. Representations of the structure of crystals of 2,2'-bi-2-imidazolinium 1,3,5-benzenetriphosphonate (H_2**BI**$^{+2}$) (H_4**BTP**$^{-2}$) • DMSO grown from DMSO. (a) View of part of a tape built from alternating bis(amidinium) dications and triphosphonate dianions linked by charge-assisted N–H···O hydrogen bonds of types $\mathbf{R_2^2(9)}$ and $\mathbf{R_2^1(7)}$. (b) View of part of a hydrogen-bonded stack of triphosphonate dianions. (c) View showing how adjacent tapes pack to create hydrogen-bonded stacks of triphosphonate dianions. (d) View along the *a* axis showing how the anionic stacks are separated by intervening bis(amidinium) dications and included molecules of DMSO. (e) Similar view with molecules of DMSO omitted. Atoms of carbon are shown in gray, hydrogen in white, nitrogen in blue, oxygen in red, phosphorus in purple, and sulfur in yellow. Hydrogen bonds are shown as broken lines.

It is noteworthy that the tapes contain two types of bis(amidinium) dications, one linked to phosphonate anions only by $\mathbf{R_2^1(7)}$ motifs and the other linked only by $\mathbf{R_2^2(9)}$ motifs. Of the four N–H···O hydrogen bonds formed by each bridging phosphonate, only those involving the neutral OH group as acceptor have N···O distances longer than 2.85 Å, suggesting that the other hydrogen bonds are strengthened by charge assistance. The increased N···O(H) distance and the corresponding bent N-H···O(H) angle presumably facilitate formation of the $\mathbf{R_2^2(9)}$ motif, which appears to be disfavored in other phosphonate salts of dication H_2**BI**$^{2+}$ for geometric reasons.

The tapes are linked by additional O–H···O hydrogen bonds between 1,3,5-benzenetriphosphonate dianions. This creates conspicuous anionic stacks aligned with the *a*

axis and held together by a total of eight O–H···O hydrogen bonds between each dianion and its two neighbors (Figure 5b). The O···O distances (2.528(11), 2.548(10), 2.603(11), and 2.657(10) Å) are normal, and most of the O–H···O angles (176, 171, 139, and 176°, respectively) are nearly linear. Large distances between the centroids of adjacent benzenetriphosphonate units within each stack (3.722(8) and 3.823(8) Å) provide no evidence of important stabilizing aromatic interactions. The anionic stacks are closely analogous to neutral hydrogen-bonded columns observed in the structure of 1,3,5-benzenetriphosphonic acid itself.[29] The overall structure of the salt (H_2**BI**$^{+2}$) (H_4**BTP**$^{-2}$) • DMSO can be described as consisting of parallel tapes of alternating hydrogen-bonded bis(amidinium) dications and triphosphonate dianions, which pack in a way that allows the dianions to form hydrogen-bonded stacks, with molecules of DMSO included in remaining spaces (Figures 5c-e).

Fluoflavinium 1,4-benzenedisulfonate (HFF$^+$)$_2$ (BDS^{-2}) • 4DMSO. Our observations suggest that protonation of bis(amidine) **BI** by acids with multiple COOH or $PO(OH)_2$ groups produces salts that crystallize to form structures in which networks of charge-assisted hydrogen bonds help position the ionic components according to established patterns. To explore the scope of this strategy, we replaced compound **BI** with fluoflavin (**FF**), a bis(amidine) closely related to tetracene. Long acenes promise to be useful as components in molecular optoelectronic devices;[30] unfortunately, however, simple hydrocarbons of this type are poorly soluble, highly reactive, and unable to engage in intermolecular interactions that can readily be used to alter properties by controlling how neighboring molecules are positioned. Fluoflavin (**FF**) and related heterocyclic compounds are attractive alternatives because substituting CH in simple acenes by N or NH creates opportunities to solubilize by

forming salts, adjust bandgaps, and control molecular organization by forming hydrogen bonds, including those assisted by charge.[31-32]

To assess this potential, we treated fluoflavin (**FF**) with various complex carboxylic, phosphonic, and sulfonic acids, but few attempts to grow crystals were successful. In one, fluoflavin (**FF**) and 1,4-benzenedisulfonic acid (H_2**BDS**) were combined in a 1:1 molar ratio in hot DMSO, and the mixture was cooled to produce crystals of composition (H**FF**$^+$)$_2$ (**BDS**$^{-2}$) • 4DMSO. Their structure was determined, and crystallographic parameters are provided in Table 2. Bis(amidine) **BI** is diprotonated by acids with values of pK_a below about 1, but fluoflavin (**FF**) is more weakly basic and is only monoprotonated by disulfonic acid H_2**BDS** in the observed structure. H**FF**$^+$ monocations are linked to bridging disulfonate dianions by charge-assisted N–H···O hydrogen bonds of type $\mathbf{R_2^2(8)}$, as shown in Figure 6a. Evidence for protonated fluoflavin H**FF**$^+$ is provided by the nearly identical lengths of the two C-N bonds incorporated in the $\mathbf{R_2^2(8)}$ motif (1.3286(19) and 1.3303(19) Å), whereas the lengths of the two other C-N bonds in the monocation are distinctly different (1.303(2) and 1.3552(19) Å). N···O distances (2.7347(15) and 2.8164(16) Å) and N–H···O angles (174°) in the salt have values that are characteristic of charge-assisted hydrogen bonds and do not support an earlier suggestion that sulfonates tend to form longer hydrogen bonds than carboxylates or phosphonates.[22] It is noteworthy that monocation H**FF**$^+$ associates with sulfonate to form an $\mathbf{R_2^2(8)}$ motif incorporating a tetrahedral O-S-O angle (111.36(6)°), whereas analogue H**BI**$^+$ prefers bifurcated $\mathbf{R_2^1(7)}$ motifs in its phosphonate salts, rather than alternative $\mathbf{R_2^2(9)}$ patterns with tetrahedral O-P-O angles. The behavior of cations H**FF**$^+$ and H**BI**$^+$ is presumably based in both cases on a preference for N–H···O angles that are nearly linear.

Table 2. Crystallographic data for salts $(H\mathbf{FF}^{+})_2$ $(\mathbf{BDS}^{-2})$ • 4DMSO and $(H_2\mathbf{FF}^{+2})$ $[PO_2(OH)_2^-]_2$ • H_2O.

salt	$(H\mathbf{FF}^{+})_2$ $(\mathbf{BDS}^{-2})$ • 4DMSO	$(H_2\mathbf{FF}^{+2})$ $[PO_2(OH)_2^-]_2$ • H_2O
crystallization medium	DMSO	heptanoic acid
formula	$C_{42}H_{50}N_8O_{10}S_6$	$C_{14}H_{18}N_4O_9P_2$
crystal system	triclinic	monoclinic
space group	$P\bar{1}$	$C2/c$
a (Å)	8.4966(4)	22.7176(15)
b (Å)	10.1445(5)	4.5011(3)
c (Å)	15.0176(7)	20.409(2)
α (°)	74.608(2)	90
β (°)	81.509(1)	122.834(2)
γ (°)	66.496(2)	90
V (Å^3)	1143.17(9)	1753.5(2)
Z	1	4
T (K)	150	150
ρ_{calc} (g cm^{-3})	1.481	1.698
μ (mm^{-1})	3.329	2.842
crystal size (mm)	0.12 × 0.12 × 0.10	0.11 × 0.07 × 0.05
θ range (°)	3.06-69.98	4.63-68.48
measured reflections	19045	37239
independent reflections	4232	1613
R_1, $I > 2\sigma(I)$	0.0360	0.0616
R_1, all data	0.0364	0.0635
wR_2, $I > 2\sigma(I)$	0.1001	0.1350
wR_2, all data	0.1006	0.1362
GoF	1.025	1.234

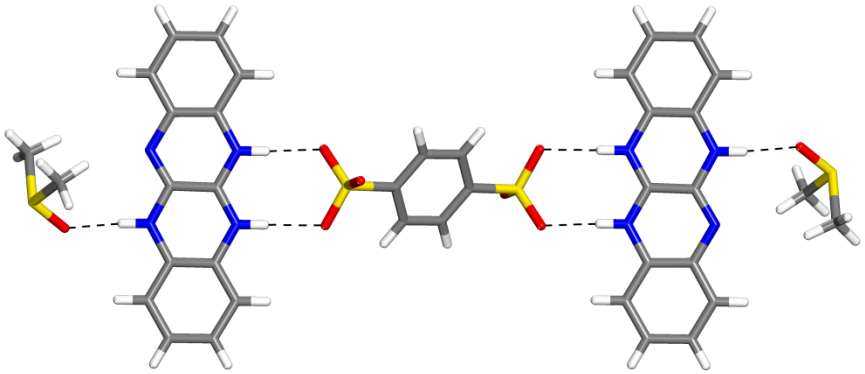

a

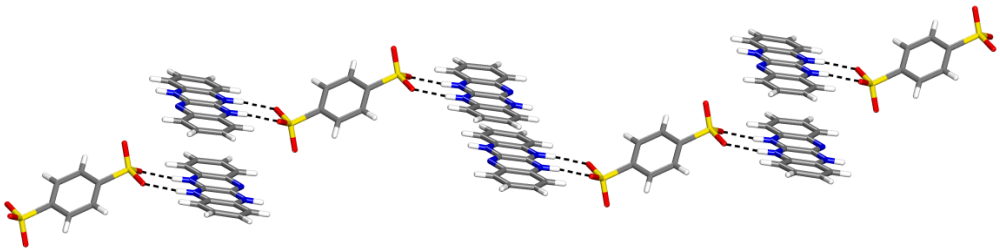

b

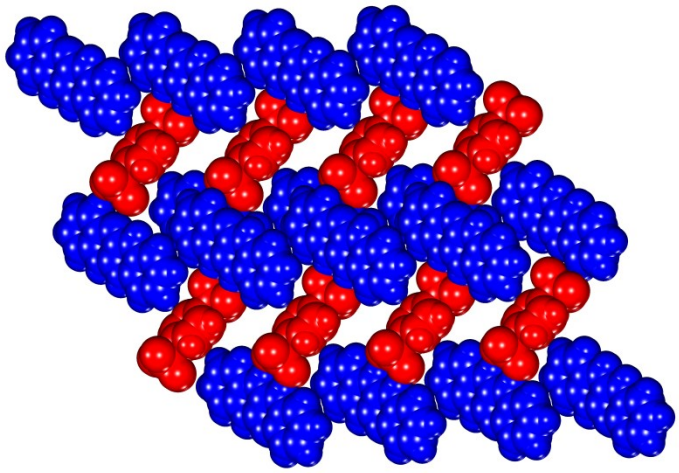

c

Figure 6. Representations of the structure of crystals of fluoflavinium 1,4-benzenedisulfonate (H**FF**$^{+}$)$_2$ (**BDS**$^{-2}$) • 4DMSO grown from DMSO. (a) View showing fluoflavinium monocations linked to a bridging disulfonate dianion by charge-assisted N–H···O hydrogen bonds of type $\mathbf{R_2^2(8)}$ and to two included molecules of DMSO by simple N–H···O hydrogen bonds. (b) View showing how the hydrogen-bonded (H**FF**$^{+}$)$_2$ (**BDS**$^{-2}$) units pack to create offset stacks of fluoflavinium monocations. (c) View showing alternating layers of fluoflavinium monocations (blue) and disulfonate dianions (red), with guest molecules of DMSO omitted for clarity. Unless otherwise indicated, atoms of carbon are shown in gray, hydrogen in white, nitrogen in blue, oxygen in red, and sulfur in yellow. Hydrogen bonds are shown as broken lines.

Carboxylate-bridged monocations H**BI**$^{+}$ are typically further linked to form tapes by N–H···N hydrogen bonds of type $\mathbf{R_2^2(10)}$, as shown in Figure 1b. In contrast, similar extended association is not observed in fluoflavinium salt (H**FF**$^{+}$)$_2$ (**BDS**$^{-2}$), presumably because it would create repulsive H···H interactions involving adjacent C-H bonds (Figure 7). Instead, H**FF**$^{+}$ monocations form additional hydrogen bonds with included molecules of DMSO (Figure 6a). The resulting hydrogen-bonded (H**FF**$^{+}$)$_2$ (**BDS**$^{-2}$) units pack to form a structure with alternating layers of disulfonate dianions and H**FF**$^{+}$ monocations stacked in offset with an interplanar separation of approximately 3.8 Å (Figures 6b and c).

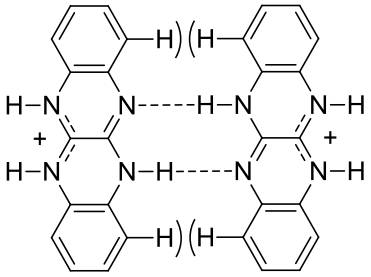

Figure 7. Representation of hypothetical repulsive H···H interactions arising when pairs of fluoflavinium monocations are linked by N–H···N hydrogen bonds of type $\mathbf{R_2^2(8)}$.

Fluoflavinium monophosphate ($H_2\mathbf{FF}^{+2}$) $[PO_2(OH)_2^-]_2 \bullet H_2O$. The failure of a sulfonic acid to diprotonate fluoflavin (**FF**) prompted us to examine stronger acids. Fluoflavin (**FF**) and pyrophosphoric acid were combined in a 1:1 molar ratio in heptanoic acid, the mixture was heated, and subsequent cooling produced crystals of a phosphate salt of composition ($H_2\mathbf{FF}^{+2}$) $[PO_2(OH)_2^-]_2 \bullet H_2O$. Phosphate is presumably introduced as a contaminant in pyrophosphate by partial hydrolysis. The structure of the salt was resolved, and Table 2 summarizes the crystallographic data. As planned, the salt incorporates $H_2\mathbf{FF}^{+2}$ dications linked to two monophosphate monoanions (in part statistically disordered over two positions) by a total of four N–H···O hydrogen bonds of type $\mathbf{R_2^2(8)}$, as shown in Figure 8a. Formation of diprotonated fluoflavin ($H_2\mathbf{FF}^{+2}$) is consistent with the observation of similar C-N distances within the $\mathbf{R_2^2(8)}$ motifs (1.321(5)-1.336(5) Å), and the N···O distances (2.641(6)-2.749(6) Å) and N–H···O angles (160-172°) are normal. Additional single O–H···O hydrogen bonds with normal O···O distances (2.701(7) Å) link the monophosphate anions to create ionic columns in which $H_2\mathbf{FF}^{+2}$ dications stack in offset with an interplanar separation of approximately 3.5 Å (Figure 8a). Monophosphate anions in adjacent columns are further linked by additional O–

H···O hydrogen bonds, some involving included molecules of H_2O (Figure 8b). The overall structure consists of alternating ionic layers, one composed of extensively hydrogen-bonded monophosphate anions and the other containing $H_2\mathbf{FF}^{+2}$ dications packed in a herringbone pattern (Figure 8c).

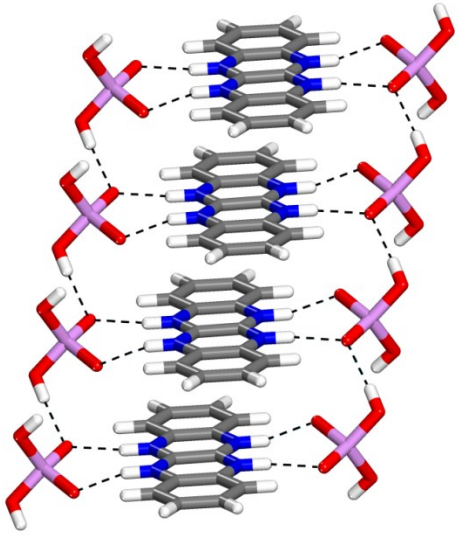

a

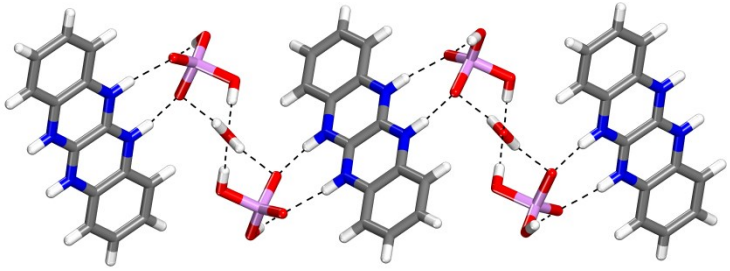

b

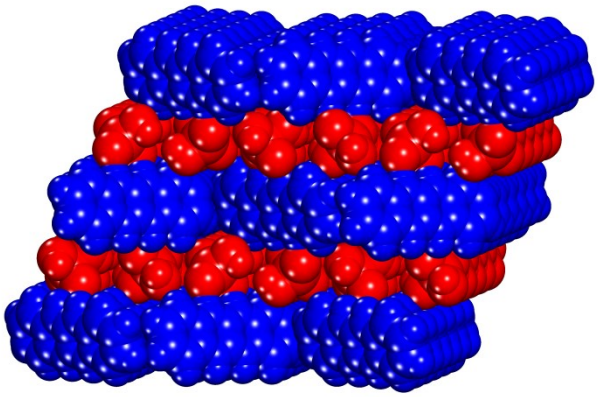

c

Figure 8. Representations of the structure of crystals of fluoflavinium monophosphate (H_2**FF**$^{+2}$) $[PO_2(OH)_2^-]_2 \bullet H_2O$ grown from heptanoic acid. (a) View showing one of two non-equivalent ionic columns composed of stacked H_2**FF**$^{+2}$ dications and monophosphate anions. Dications are linked to monoanions by charge-assisted N–H···O hydrogen bonds of type $\mathbf{R_2^2(8)}$, and monoanions are further connected by O–H···O hydrogen bonds. (b) View showing how adjacent columns are linked by additional O–H···O hydrogen bonds involving monophosphate anions and included molecules of H_2O. (c) View showing alternating ionic layers of monophosphate anions (red) and H_2**FF**$^{+2}$ dications (blue) packed in a herringbone motif, with guest molecules of H_2O omitted for clarity. Unless otherwise indicated, atoms of carbon are shown in gray, hydrogen in white, nitrogen in blue, oxygen in red, and phosphorus in purple. Hydrogen bonds are shown as broken lines.

Conclusions

2,2'-Bi-2-imidazoline (**BI**) is known to react with compounds containing multiple COOH groups to give carboxylate salts that crystallize as ionic networks held together in part by characteristic charge-assisted N-H···O hydrogen bonds of type $\mathbf{R_2^2(9)}$. Typical carboxylic acids are only acidic enough to produce salts of monocation H**BI**$^+$. In contrast, phosphonic acids and sulfonic acids are expected to be strong enough to reliably produce salts of dication H_2**BI**$^{+2}$. As intended, mixing bis(amidine) **BI** with 1,4-benzenediphosphonic acid and 1,3,5-benzenetriphosphonic acid yielded crystals of phosphonate salts of dication H_2**BI**$^{+2}$. Structural analyses showed that such salts tend to incorporate tapes composed of alternating dications and anions linked by multiple charge-assisted N-H···O hydrogen bonds of type $\mathbf{R_2^2(9)}$ and $\mathbf{R_2^1(7)}$. Typically, the tapes are further connected to form sheets or other assemblies by additional O-H···O hydrogen bonding of phosphonate anions. Fluoflavin (**FF**), a more weakly basic analogue of bis(amidine) **BI**, reacted with 1,4-benzenedisulfonic acid to produce crystals of a salt of monoprotonated cation H**FF**$^+$. However, diprotonation could be achieved by treatment with phosphoric acid, which gave crystals incorporating H_2**FF**$^{+2}$ dications linked to phosphate anions by charge-assisted N-H···O hydrogen bonds of type $\mathbf{R_2^2(8)}$. These observations, along with recent related studies,[4] demonstrate that salts produced by reactions of bis(amidines) with complex carboxylic, phosphonic, and sulfonic acids yield crystals with structural features resulting predictably from the geometry of the ions and their ability to engage in multiple charge-assisted hydrogen bonds according to standard patterns.

Experimental Section

General Notes. 2,2'-Bi-2-imidazoline (**BI**),[5] fluoflavin (**FF**),[10] and 1,4-benzenedisulfonic acid (H_2**BDS**)[14] were prepared by published methods. Ethyl esters of diphosphonic acid H_4**BDP** and triphosphonic acid H_6**BTP** were made by reported procedures[11] and converted into the corresponding acids by hydrolysis under standard conditions.[12,13] Other compounds were purchased from commercial sources and used without further purification.

Syntheses and Characterizations of Salts

Separate solutions of 2,2'-bi-2-imidazoline (**BI**) and various phosphonic acids were prepared in 3:2 EtOH/H_2O or DMSO. The solutions were filtered, mixed in various molar ratios (1:1 for H_4**BDP** or 3:2 for H_6**BTP**), and kept at 25 °C to allow crystallization to occur. Fluoflavin (**FF**) and either disulfonic acid H_2**BDS** or pyrophosphoric acid were combined in a 1:1 ratio, a small volume of solvent was added (DMSO for H_2**BDS** or heptanoic acid for pyrophosphoric acid), and the resulting mixture was stirred and heated briefly until the solids had dissolved. Crystallization occurred while the resulting solution was kept at 25 °C.

2,2'-Bi-2-imidazolinium 1,4-benzenediphosphonate (H_2BI^{+2}) (H_2BDP^{-2}). Isolated in 6% yield as colorless air-stable crystals: ^{1}H NMR (700 MHz, D_2O) δ 3.95 (s, 8H), 7.64 (m, 4H); ^{13}C NMR (175 MHz, D_2O) δ 45.9, 129.9, 137.2 (d, $^1J_{CP}$ = 174 Hz), 152.5; ^{31}P NMR (283

MHz, D_2O) δ 12.4; HRMS (+ESI) calcd. for $C_6H_{12}N_4^{+2}$ *m/e* 70.05310, found 70.02919; HRMS (-ESI) calcd. for $C_6H_7O_6P_2^-$ *m/e* 236.97179, found 236.97653.

2,2'-Bi-2-imidazolinium 1,4-benzenediphosphonate (H_2BI^{+2}) (H_2BDP^{-2}) • 2DMSO. Isolated along with the unsolvated form as colorless air-stable crystals.

2,2'-Bi-2-imidazolinium 1,4-benzenediphosphonate (H_2BI^{+2}) (H_2BDP^{-2}) • $4H_2O$. Isolated in 47% yield as colorless air-stable crystals: mp > 250 °C (dec); FTIR (ATR) 3300-2500 (br), 1598, 1576, 1290, 1127, 1058, 897 cm^{-1}; ^1H NMR (700 MHz, D_2O) δ 3.91 (s, 8H), 7.63 (m, 4H); ^{31}P NMR (283 MHz, D_2O) δ 12.32; HRMS (+ESI) calcd. for $C_6H_{12}N_4^{+2}$ *m/e* 70.05310, found 70.02919; HRMS (-ESI) calcd. for $C_6H_7O_6P_2^-$ *m/e* 236.97179, found 236.97222. Anal. Calcd for $C_{12}H_{26}N_4O_{10}P_2$: C, 32.13; H, 5.85; N, 12.50. Found: C, 32.82; H, 5.57; N, 12.49.

2,2'-Bi-2-imidazolinium 1,3,5-benzenetriphosphonate (H_2BI^{+2}) (H_4BTP^{-2}) • DMSO. Isolated in 34% yield as colorless air-stable crystals: mp > 200 °C (dec); FTIR (ATR) 3200-2100 (br), 1600, 1572, 1289, 1131, 938 cm^{-1}; ^1H NMR (700 MHz, D_2O) δ 2.55 (s, 6H), 3.89 (s, 8H), 8.00 (s, 3H); ^{31}P NMR (283 MHz, D_2O) δ 12.2; HRMS (+ESI) calcd. for $C_6H_{12}N_4^{+2}$ *m/e* 70.05310, found 70.02980; HRMS (-ESI) calcd. for $C_6H_8O_9P_3^-$ *m/e* 316.93812, found 316.94431.

Fluoflavinium 1,4-benzenedisulfonate ($HFF^+)_2$ (BDS^{-2}) • 4DMSO. FTIR (ATR) 3000 (br), 1694, 1556, 1486, 1232, 1126, 1023, 997 cm^{-1}; HRMS (-ESI) calcd. for $C_6H_6O_6S_2^{-2}$ *m/e*

118.98029, found 118.97143. Anal. Calcd for $C_{34}H_{26}N_8O_6S_2$ • 4DMSO: C, 49.50; H, 4.95; N, 11.00; S, 18.84. Found: C, 48.84; H, 4.80; N, 10.86; S, 18.51.

Fluoflavinium monophosphate (H_2FF^{+2}) $[PO_2(OH)_2^-]_2$ • H_2O. Isolated in amounts insufficient for extensive characterization.

X-Ray Crystallography

Structural analyses of single crystals were carried out in one of two ways: (1) At 150 K with a Bruker AXS X8/Proteum Microstar diffractometer, using Cu Kα radiation produced by an FR591 rotating-anode generator equipped with multilayer HELIOS optics (all salts except for (H_2**BI**$^{+2}$) (H_2**BDP**$^{-2}$) and (H_2**BI**$^{+2}$) (H_2**BDP**$^{-2}$) • $4H_2O$); or (2) at 100 K using a Bruker APEX diffractometer equipped with an Incoatec microsource generator. Collections of data and determinations of initial unit-cell lattice parameters were performed with the *APEX2* suite of software, final lattice parameters and integrated intensities were calculated using *SAINT* software,[33] and a multi-scan absorption correction was applied using *SADABS*.[34] Structures were solved with SHELXS-97 and refined with SHELXL-97.[35] All non-hydrogen atoms were refined with anisotropic thermal displacement parameters. Hydrogen atoms were first located from the calculated difference-Fourier maps, then refined as riding atoms using the standard models from SHELXL-97. In all structures with included DMSO, the guest molecules were found to be disordered. Also disordered were included H_2O and $PO_2(OH)_2^-$ in the salt (H_2**FF**$^{+2}$) $[PO_2(OH)_2^-]_2$ • H_2O, the H_2**BDP**$^{-2}$ dianion in the salt (H_2**BI**$^{+2}$) (H_2**BDP**$^{-2}$) • 2DMSO, and one phosphonate group in the salt (H_2**BI**$^{+2}$) (H_4**BTP**$^{-2}$) • DMSO. Structural analysis of the

salt (H_2**BI**$^{+2}$) (H_4**BTP**$^{-2}$) • DMSO is of lower quality than the others because the crystals were twinned and decomposed, leading to truncation of the collection of final data.

When sufficient amounts of crystalline material were available, assessments of homogeneity were carried out by comparing calculated diffraction patterns (generated using Mercury software)[36] with experimental patterns measured on a Bruker D8 Discover diffractometer with copper radiation (CuKα, λ = 1.5418 Å). For the three samples analyzed in this way, calculated and experimental patterns were closely similar.[37]

Acknowledgments. We are grateful to the Natural Sciences and Engineering Research Council of Canada, the Ministère de l'Éducation du Québec, the Canada Foundation for Innovation, the Canada Research Chairs Program, and Université de Montréal for financial support. In addition, we thank Daniel Beaudoin for helpful advice about phosphonic and sulfonic acids.

Supporting Information Available. Additional crystallographic details (tables of structural data in CIF format, thermal atomic displacement ellipsoid plots, and comparisons of calculated and experimental powder diffraction patterns). This information is available free of charge via the Internet at http://pubs.acs.org/.

Notes and References

1. Wuest, J. D. *Chem. Commun.* **2005**, 5830-5837.
2. Hosseini, M. W. *Acc. Chem. Res.* **2005**, *38*, 313-323.
3. Ward, M. D. *Struct. Bonding (Berlin)* **2009**, *132*, 1-23.
4. Lie, S.; Maris, T.; Malveau, C.; Beaudoin, D.; Helzy, F.; Wuest, J. D. *Cryst. Growth Des*. **2013**, *13*, 1872-1877.
5. Wang, J. C.; Bauman, J. E., Jr. *Inorg. Chem.* **1965**, *4*, 1613-1615.
6. Bernstein, J.; Davis, R. E.; Shimoni, L.; Chang, N.-L. *Angew. Chem., Int. Ed.* **1995**, *34*, 1555-1573.
7. Jaffé, H. H.; Freedman, L. D.; Doak, G. O. *J. Am. Chem. Soc.* **1953**, *75*, 2209-2211.
8. Dong, H.; Du, H.; Wickramasinghe, S. R.; Qian, X. *J. Phys. Chem. B* **2009**, *113*, 14094-14101.
9. Kong, D.; Yao, J.; Clearfield, A.; Zon, J. *Cryst. Growth Des.* **2008**, *8*, 2892-2898.
10. Kaupp, G.; Naimi-Jamal, M. R. *Eur. J. Org. Chem.* **2002**, 1368-1373.
11. Hirao, T.; Masunaga, T.; Yamada, N.; Ohshiro, Y.; Agawa, T. *Bull. Chem. Soc. Jpn.* **1982**, *55*, 909–913.
12. Kong, D.; Clearfield, A.; Zoń, J. *Cryst. Growth Des.* **2005**, *5*, 1767-1773.
13. Kong, D.; Yao, J.; Clearfield, A.; Zon, J. *Cryst. Growth Des.* **2008**, *8*, 2892-2898.
14. Mietrach, A.; Muesmann, T. W. T.; Christoffers, J.; Wickleder, M. S. *Eur. J. Inorg. Chem.* **2009**, 5328-5334.
15. Kraft, A. *J. Chem. Soc., Perkin Trans. 1* **1999**, 705-714.

16. Annamalai, V. R.; Linton, E. C.; Kozlowski, M. C. *Org. Lett.* **2009**, *11*, 621-624.

17. Piskov, V. B.; Kasperovich, V. P. *Zh. Org. Khim.* **1978**, *14*, 820-834.

18. Elguero, J.; Gonzalez, É.; Imbach, J.-L.; Jacquier, R. *Bull. Soc. Chim. Fr.* **1969**, 4075-4077.

19. Kong, D.; McBee, J. L.; Clearfield, A. *Cryst. Growth. Des.* **2005**, *5*, 643-649.

20. Liang, Z.; Wang, F.; Wu, Q.; Zhi, X.; Pan, Q. *Acta Crystallogr*. **2011**, *E67*, m1399.

21. Guo, Y.-C.; Chen, S.-Y.; Bao, X.-Y.; Qiu, D.-F.; Feng, Y.-Q. *Chinese J. Struct. Chem*. **2011**, *30*, 1791-1797.

22. For a comparison of N-H···O hydrogen bonds in salts of carboxylates, phosphonates, and sulfonates, see: Pirard, B.; Baudoux, G.; Durant, F. *Acta Crystallogr*. **1995**, *B51*, 103-107.

23. Taylor, R.; Kennard, O. *Acc. Chem. Res.* **1984**, *17*, 320-326.

24. Taylor, R.; Kennard, O.; Versichel, W. *Acta Crystallogr*. **1984**, *B40*, 280-288.

25. Ferguson, G.; Glidewell, C.; Gregson, R. M.; Meehan, P. R. *Acta Crystallogr.* **1998**, *B54*, 129-138.

26. Mehring, M. *Eur. J. Inorg. Chem.* **2004**, 3240-3246.

27. Murugavel, R.; Singh, M. P. *New J. Chem.* **2010**, *34*, 1846-1854.

28. Białek, M. J.; Zaręba, J. K.; Janczak, J.; Zoń, J. *Cryst. Growth. Des.* **2013**, *13*, 4039-4050.

29. Hix, G. B.; Caignaert, V.; Rueff, J.-M.; Le Pluart, L.; Warren, J. E.; Jaffrès, P.-A. *Cryst. Growth Des.* **2007**, 7, 208-211.

30. Anthony, J. E. *Angew. Chem., Int. Ed.* **2008**, *47*, 452-483.

31. Lindner, B. D.; Engelhart, J. U.; Märken, M.; Tverskoy, O.; Appleton, A. L.; Rominger, F.; Hardcastle, K. I.; Enders, M.; Bunz, U. H. F. *Chem. Eur. J.* **2012**, *18*, 4627-4633.

32. Tong, C.; Zhao, W.; Luo, J.; Mao, H.; Chen, W.; Chan, H. S. O.; Chi, C. *Org. Lett.* **2012**, *14*, 494-497.

33. *APEX2* and *SAINT*, *Version 7.68A*; Bruker AXS Inc.: Madison, WI 53719-1173, 2009.

34. Sheldrick, G. M., *SADABS*, *Version 2008/1*; Bruker AXS Inc.: Madison, WI 53719-1173, 2008.

35. Sheldrick, G. M. *Acta Crystallogr*. **2008**, *A64*, 112-122.

36. Macrae, C. F.; Bruno, I. J.; Chisholm, J. A.; Edgington, P. R.; McCabe, P.; Pidcock, E.; Rodriguez-Monge, L.; Taylor, R.; van de Streek, J.; Wood, P. A. *J. Appl. Cryst*. **2008**, *41*, 466-470.

37. For details, see the Supporting Information.

For Table of Contents Use Only

Table of Contents Graphic

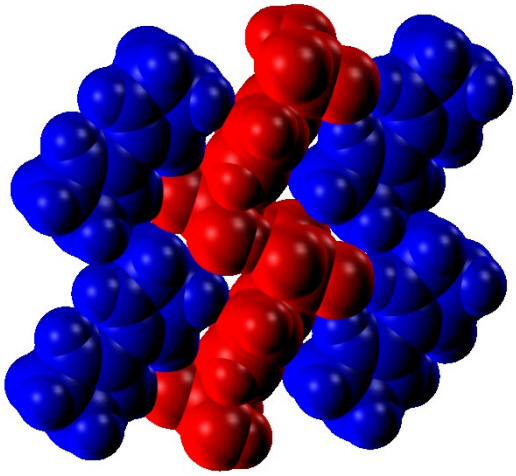

Table of Contents Synopsis

Salts produced by treating 2,2'-bi-2-imidazoline and a related bis(amidine), fluoflavin, with complex phosphonic acids and sulfonic acids yield crystals with structural features resulting predictably from the geometry of the ions and their ability to engage in multiple charge-assisted hydrogen bonds according to standard patterns.

3.8 Contributions of Co-Authors

The principal author synthesized and characterized the compounds presented in this manuscript, and she obtained them in crystalline form. In addition, she wrote the corresponding parts of the first draft of the manuscript that will be submitted for publication and forms the body of Chapter 3. Thierry Maris determined the structure of the crystals by X-ray diffraction, and he also contributed to the manuscript by preparing illustrations and by proof-reading initial drafts. James D. Wuest supervised the research and contributed to writing the manuscript.

4.0 Chapter 4: Conclusion

4.1 Conclusions and Future Work

New molecular materials can be designed effectively by the strategy of molecular tectonics. Molecules used in this approach possess the ability to recognize one another using various non-covalent intermolecular interactions. The topology of the molecules, together with the strength and directionality of the interactions between them, controls the overall molecular organization. Hydrogen bonds are among the most effective interactions, and they can be further strengthened by incorporating electrostatic interactions between components of opposite charge.

We have studied this effect in new molecular networks incorporating charge-assisted hydrogen bonds based on the association of cations derived from a bis(amidine), 2,2'-bi-2-imidazoline, with anions derived from carboxylic acids and phosphonic acids, all containing multiple COOH or $PO(OH)_2$ groups. We have also examined related networks constructed from cations derived from a second bis(amidine), fluoflavin, and anions derived from a disulfonic acid and phosphoric acid. In our studies, emphasis was placed on how the geometry and pK_a values of the acids can be varied in order to generate different molecular structures. As expected, protonation of 2,2'-bi-2-imidazoline and fluoflavin by the various acids occurred due to the large differences in pK_a values between the bis(amidininium) cations and the acids. X-ray diffraction studies confirmed the formation of structures incorporating multiple charge-assisted hydrogen bonds between the different components.

In all salts derived from 2,2'-bi-2-imidazoline, the geometry of the components and the nature of the preferred hydrogen-bonding motifs was found to lead to the formation of tapes, which then packed to form sheets, with the assistance of additional inter-tape hydrogen bonds in certain cases. The pK_a value of the acid involved determined the extent of proton transfer, and this had a direct impact on the type of tape formed. Only when the acids had pK_a values below about 1 did double protonation of 2,2'-bi-2-imidazoline occur to give a bis(amidinium) dication. This led to the formation of tapes consisting of alternating dications and dianions. With weaker acids, only monoprotonation occurred; consequently, alternating tapes composed of pairs of bis(amidinium) monocations linked to dianions were found in the structures.

Fluoflavin proved to be a weaker base than 2,2'-bi-2-imidazoline, and it was only monoprotonated by a disulfonic acid. Self-association of the monocation to form hydrogen-bonded pairs, such as those formed by the corresponding monoprotonated derivative of 2,2'-bi-2-imidazoline, was not observed, presumably because it is blocked by repulsive interactions involving C-H bonds adjacent to the amidine units. However, fluoflavin was found to be doubly protonated by phosphoric acid, leading to the expected formation of tapes held together by charge-assisted hydrogen bonds. Our work confirms that the association of bis(amidines) with acids provides a simple and efficient way to create networks assembled through charge-assisted hydrogen bonds.

The present work sets the stage for the future exploration of other bis(amidines) and acids with more complex geometries. An additional opportunity resides in exploiting the planarity of such components by using them to form well-ordered 2D nanopatterns adsorbed on suitable surfaces. Studies in this direction have already been undertaken and the results have shown that the molecules possess an affinity for adsorption on graphite and are able to generate predictable patterns of association with carboxylic acids. Comparison of the 3D and 2D organizations will help reveal the origin of the preferred modes of association of these compounds.

Together, all these studies will provide a deeper understanding of how charge-assisted hydrogen bonding can be used to direct molecular organization. Our work is the starting point for the creation of more intricate networks incorporating molecular components specifically chosen to give the resulting materials desirable features and properties.

Annexe 1: Chapter 2 Supporting Information

Supporting Information

Molecular Networks Created by Charge-Assisted Hydrogen Bonding in Carboxylate Salts of a Bis(amidine)

Sharon Lie, Thierry Maris, Cédric Malveau, Daniel Beaudoin, Fatima Helzy, and James D. Wuest*

Département de Chimie, Université de Montréal, Montréal, Québec H3C 3J7 Canada

Contents **Page**

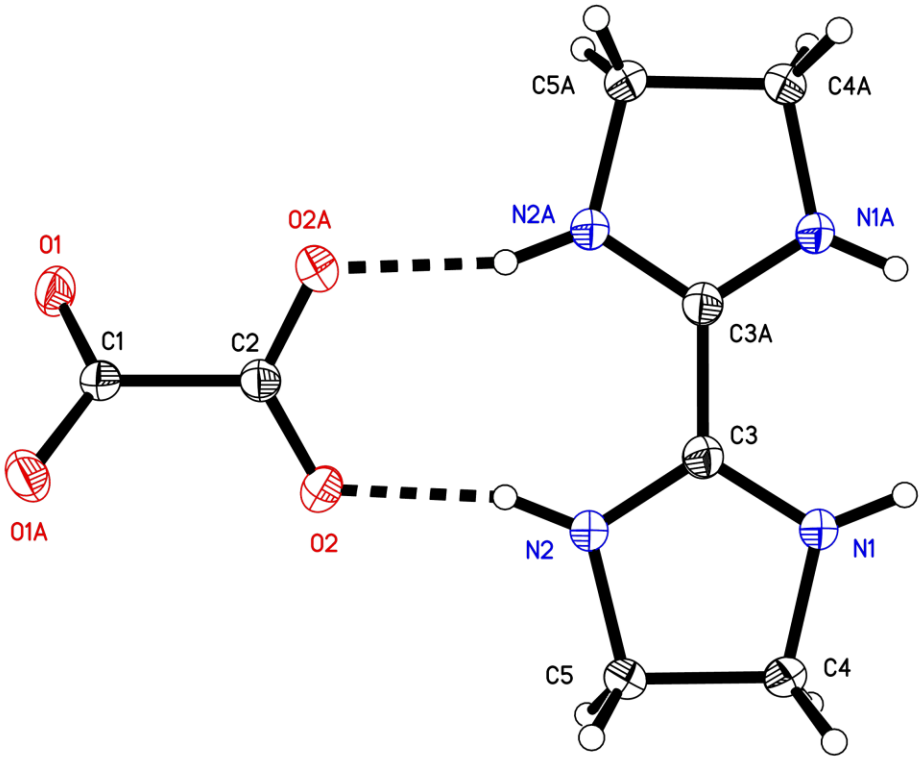

Figure S1. Thermal atomic displacement ellipsoid plot of the structure of crystals of (**BI**/H_2^{+2}) (**OA**$^{-2}$) grown from DMSO. The ellipsoids of non-hydrogen atoms are drawn at the 50% probability level, and hydrogen atoms are represented by a sphere of arbitrary size. Hydrogen bonds are shown as dotted lines. Atoms labelled with a suffix A are generated by the symmetry operation *-x+1, y, -z+3/2*.

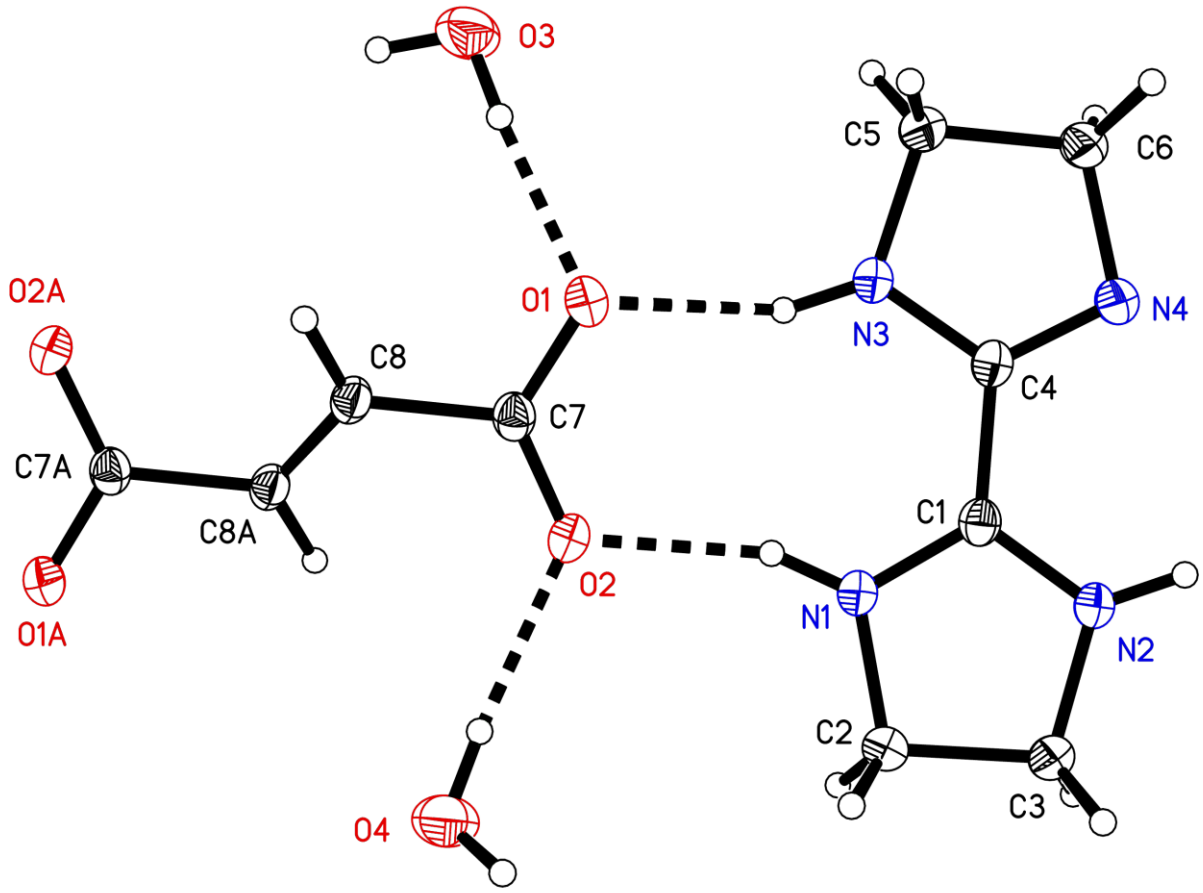

Figure S2. Thermal atomic displacement ellipsoid plot of the structure of crystals of (**BI**/H^+)$_2$ (**FA**$^{-2}$) • 4H_2O grown from DMSO. The ellipsoids of non-hydrogen atoms are drawn at the 50% probability level, and hydrogen atoms are represented by a sphere of arbitrary size. Hydrogen bonds are shown as dotted lines. Atoms labelled with a suffix A are generated by the symmetry operation *-x, -y+1, -z.*

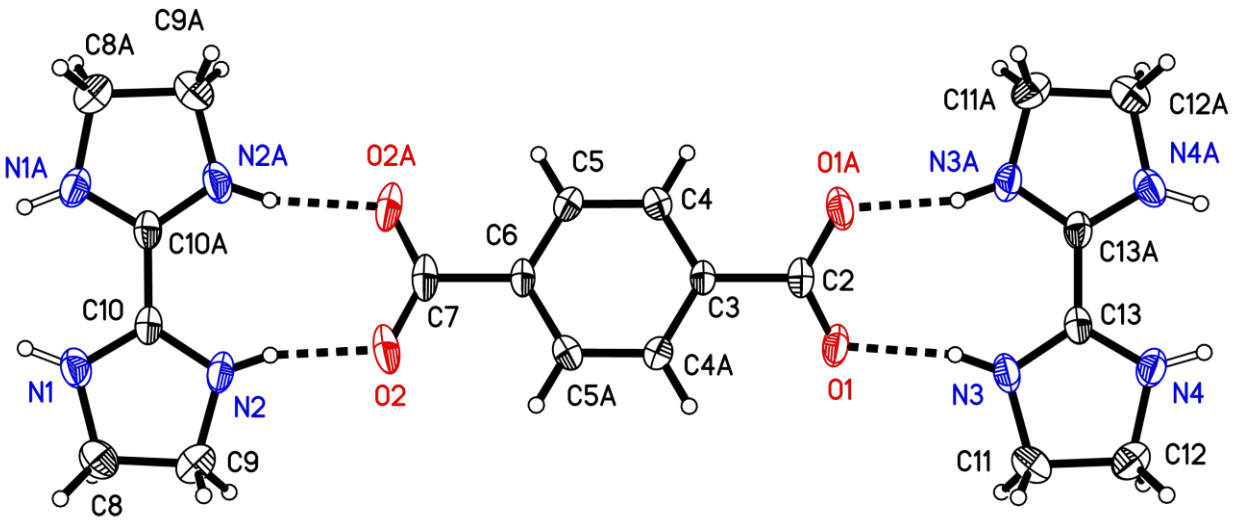

Figure S3. Thermal atomic displacement ellipsoid plot of the structure of crystals of (**BI**/H^+)$_2$ (**TA**$^{-2}$) grown from DMSO. The ellipsoids of non-hydrogen atoms are drawn at the 50% probability level, and hydrogen atoms are represented by a sphere of arbitrary size. Hydrogen bonds are shown as dotted lines. Atoms labelled with a suffix A are generated by the symmetry operation *-x, y, -z+1/2*.

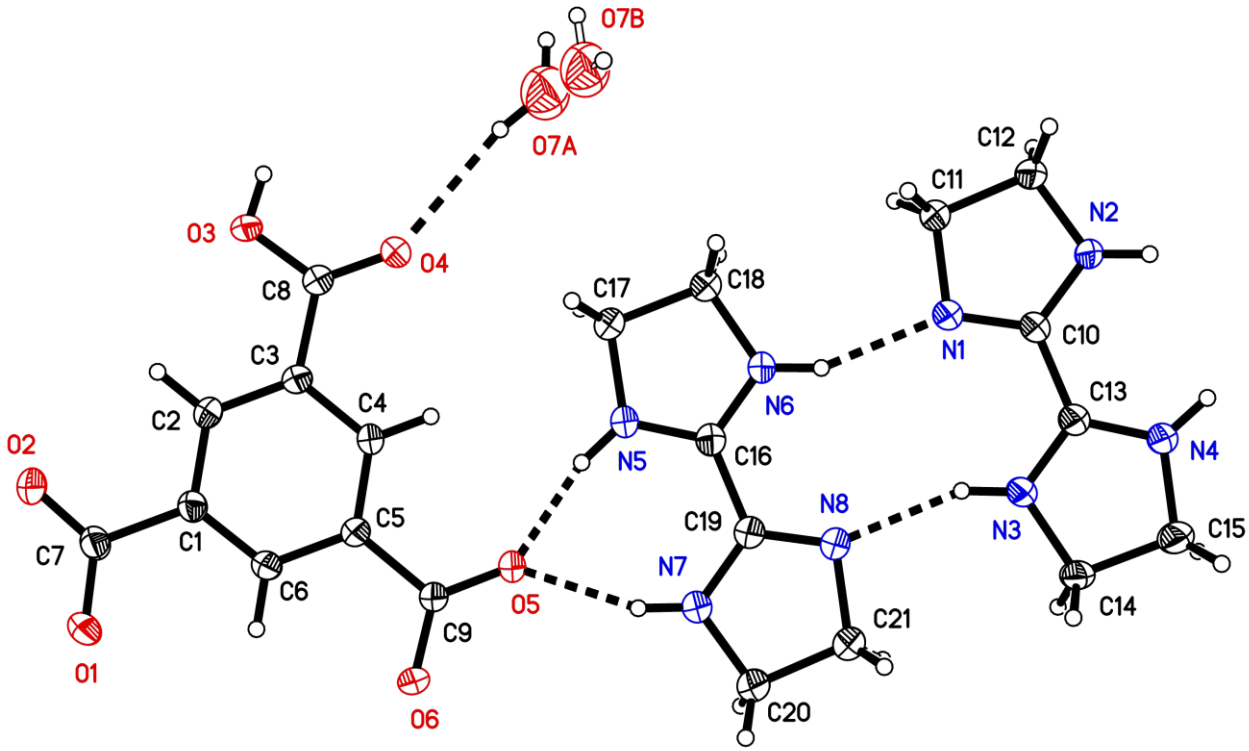

Figure S4. Thermal atomic displacement ellipsoid plot of the structure of crystals of (**BI**/H^{+})$_2$ (**TMA**/H^{-2}) • H_2O grown from DMSO. The ellipsoids of non-hydrogen atoms are drawn at the 50% probability level, and hydrogen atoms are represented by a sphere of arbitrary size. Hydrogen bonds are shown as dotted lines. The two positions for the statistically disordered water molecules are shown with labels O7A and O7B.

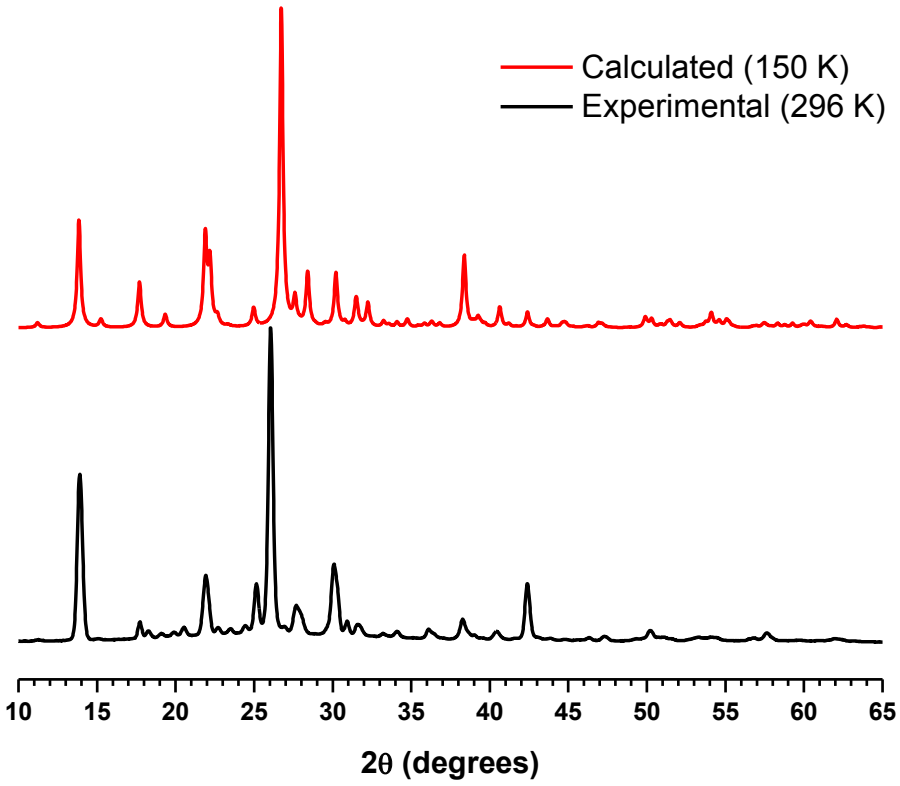

Figure S5. Comparison of calculated and experimental X-ray powder diffraction patterns for crystals of (**BI**/H_2^{+2}) (**OA**$^{-2}$) grown from DMSO.

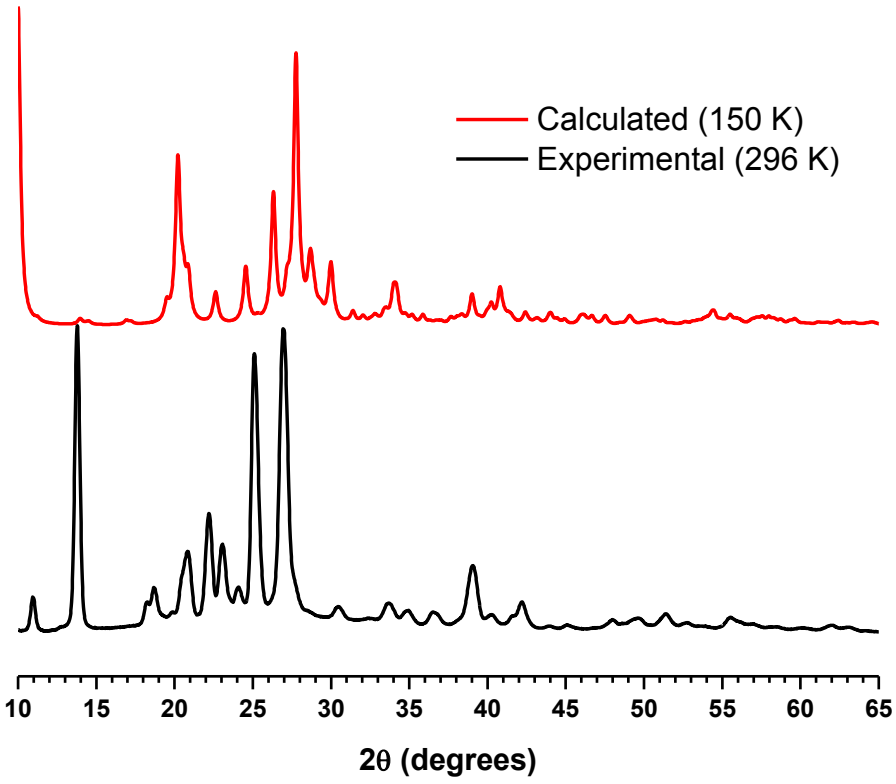

Figure S6. Comparison of calculated and experimental X-ray powder diffraction patterns for crystals of (**BI**/H^{+})$_2$ (**FA**$^{-2}$) • 4H_2O grown from DMSO.

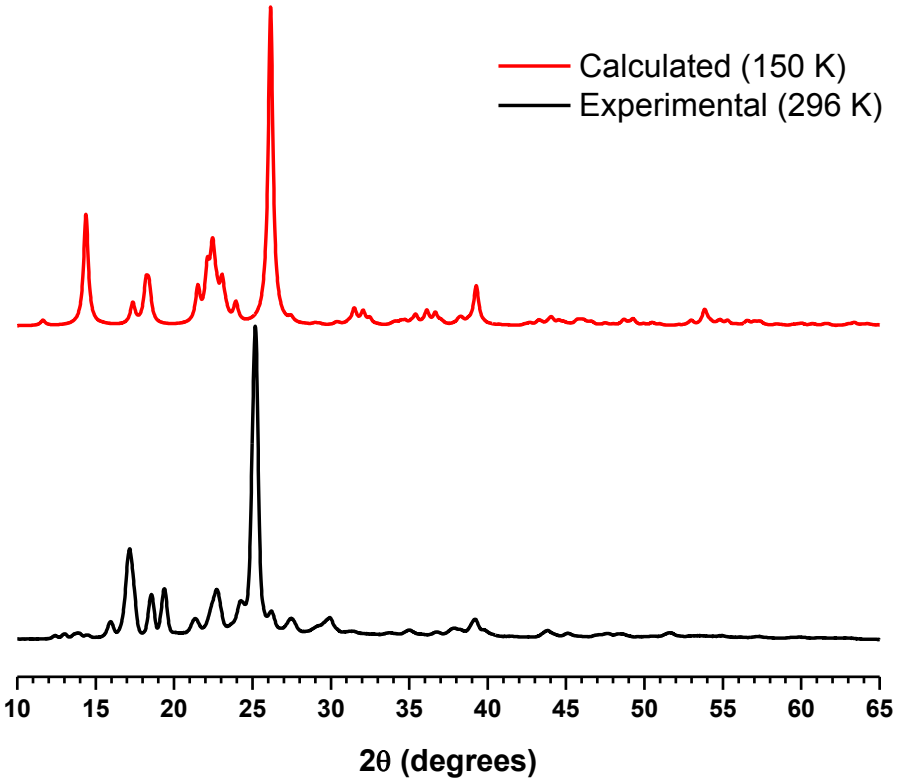

Figure S7. Comparison of calculated and experimental X-ray powder diffraction patterns for crystals of (**BI**/H^+)$_2$ (**TA**$^{-2}$) grown from DMSO.

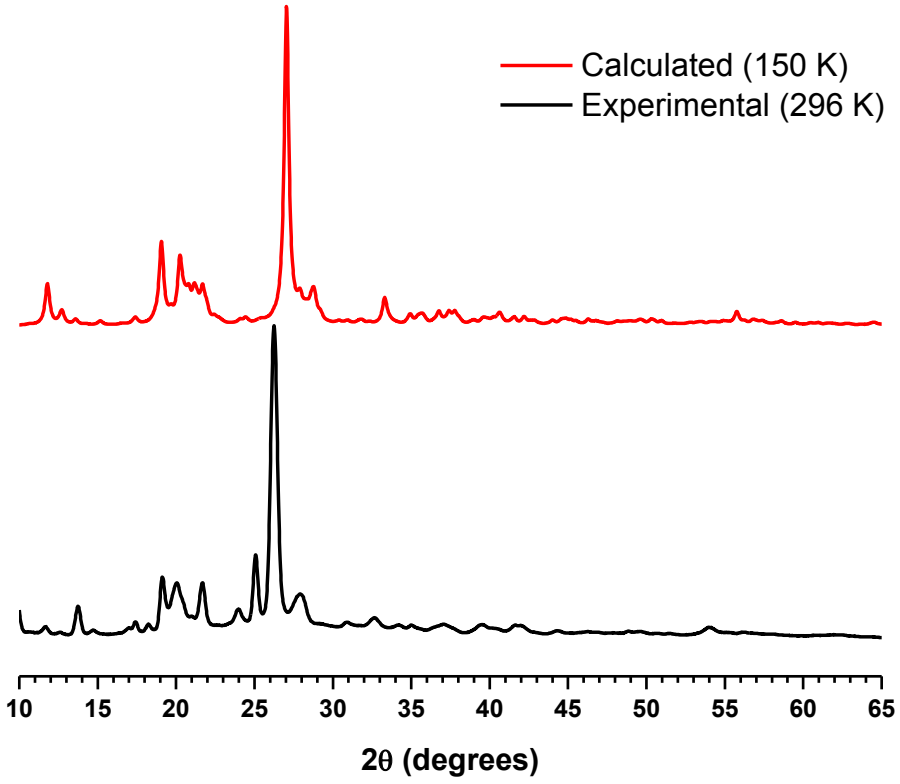

Figure S8. Comparison of calculated and experimental X-ray powder diffraction patterns for crystals of (**BI**/H^{+})$_2$ (**TMA**/H^{-2}) • H_2O grown from DMSO.

Annexe 2: Chapter 3 Supporting Information

Supporting Information

Molecular Networks

Created by Charge-Assisted Hydrogen Bonding

in Phosphonate, Phosphate, and Sulfonate Salts of Bis(amidines)

Sharon Lie, Thierry Maris, and James D. Wuest*

Département de Chimie, Université de Montréal, Montréal, Québec H3C 3J7

Canada

Contents **Page**

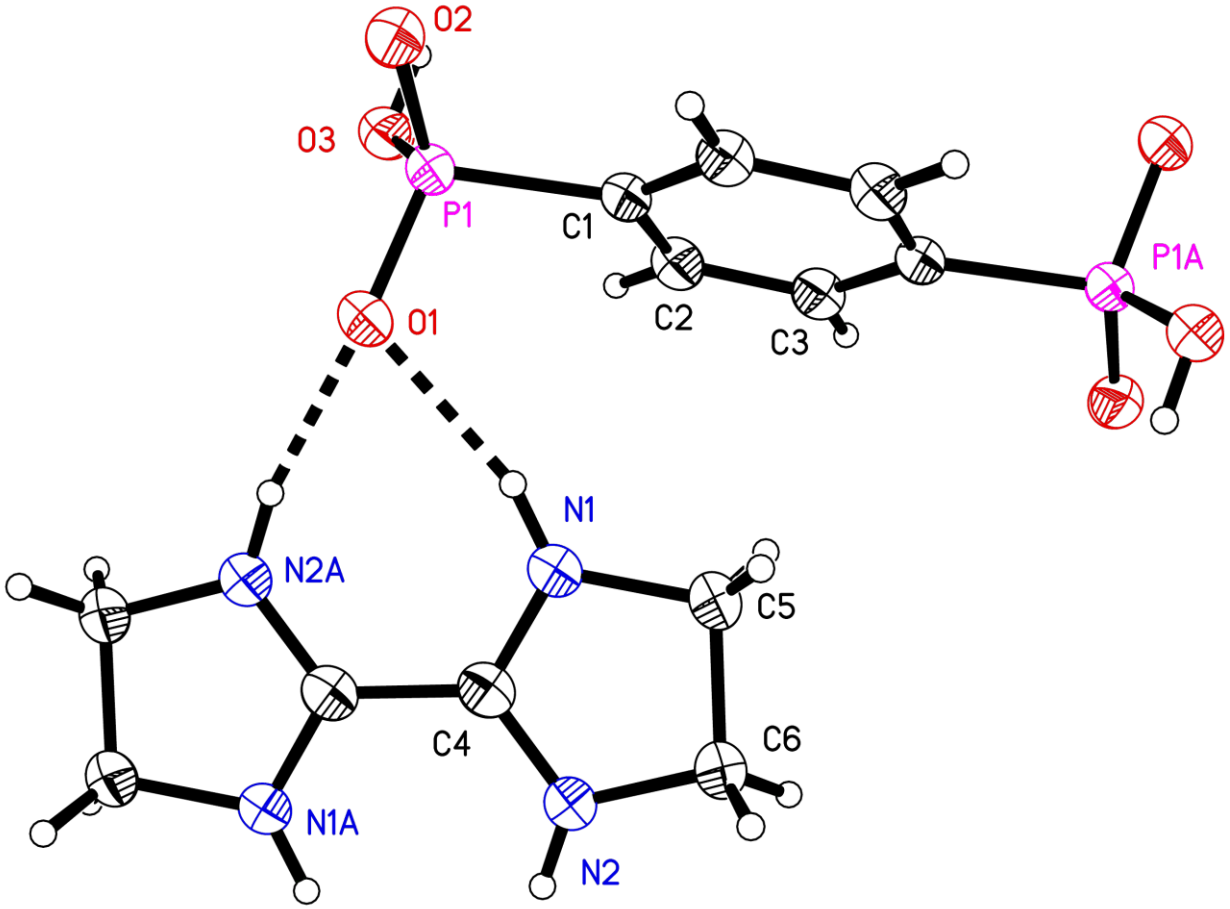

Figure S1. Thermal atomic displacement ellipsoid plot of the structure of crystals of (H_2**BI**$^{+2}$) (H_2**BDP**$^{-2}$) grown from DMSO. The ellipsoids of non-hydrogen atoms are drawn at the 50% probability level, and hydrogen atoms are represented by a sphere of arbitrary size. Hydrogen bonds are shown as dotted lines.

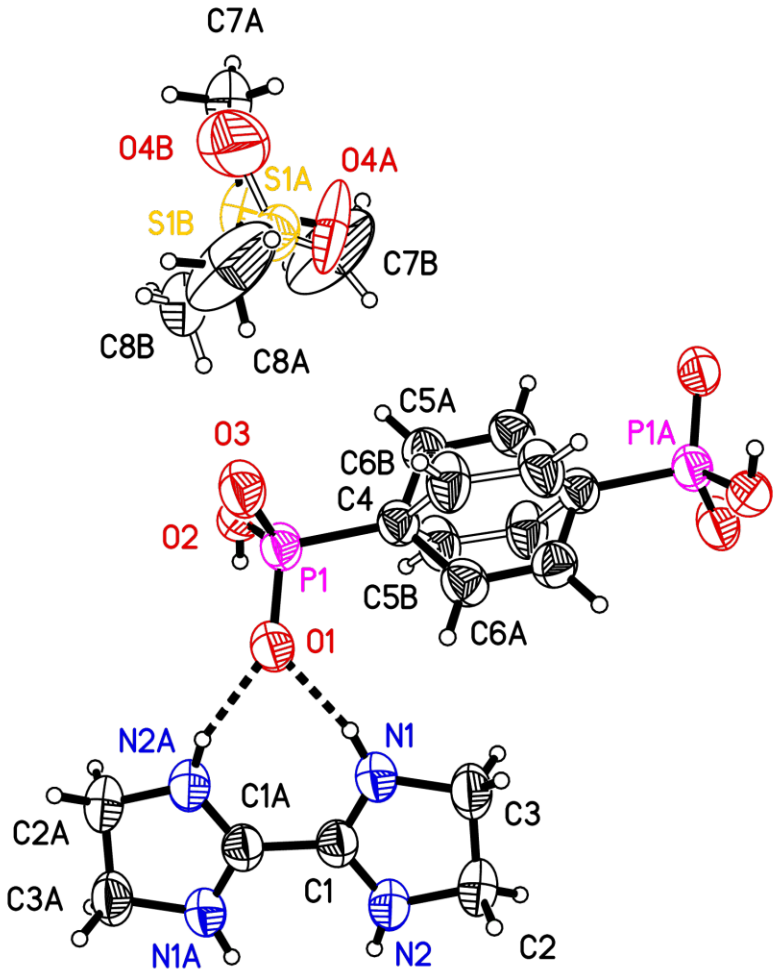

Figure S2. Thermal atomic displacement ellipsoid plot of the structure of crystals of (H_2**BI**$^{+2}$) (H_2**BDP**$^{-2}$) • 2DMSO grown from DMSO. The ellipsoids of non-hydrogen atoms are drawn at the 50% probability level, and hydrogen atoms are represented by a sphere of arbitrary size. Hydrogen bonds are shown as dotted lines. Atoms labeled with the suffix B are from the second part of the statistically disordered fragments.

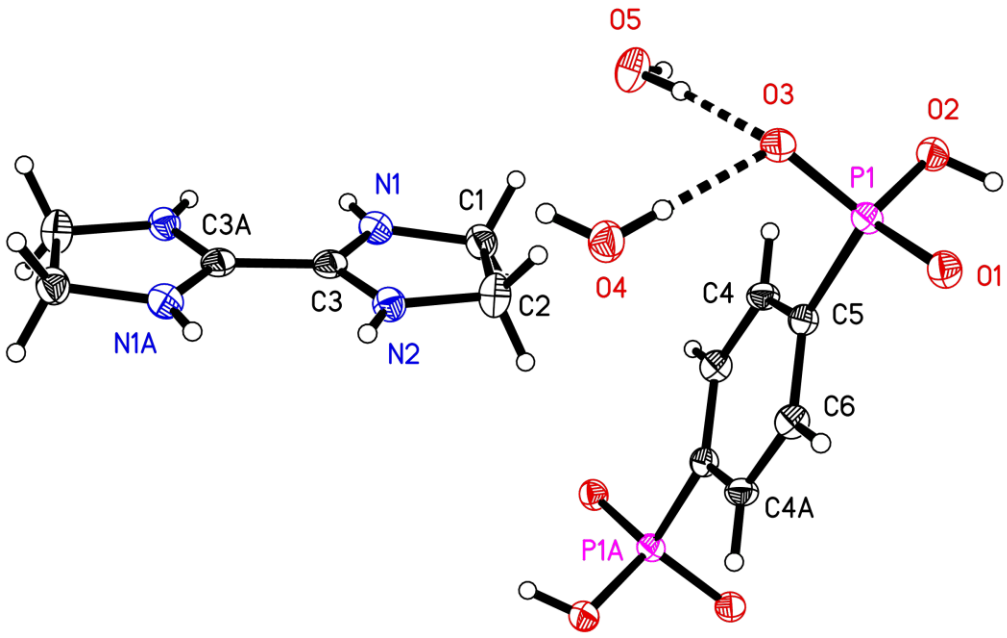

Figure S3. Thermal atomic displacement ellipsoid plot of the structure of crystals of (H_2**BI**$^{+2}$) (H_2**BDP**$^{-2}$) • 4H_2O grown from EtOH/H_2O. The ellipsoids of non-hydrogen atoms are drawn at the 50% probability level, and hydrogen atoms are represented by a sphere of arbitrary size. Hydrogen bonds are shown as dotted lines.

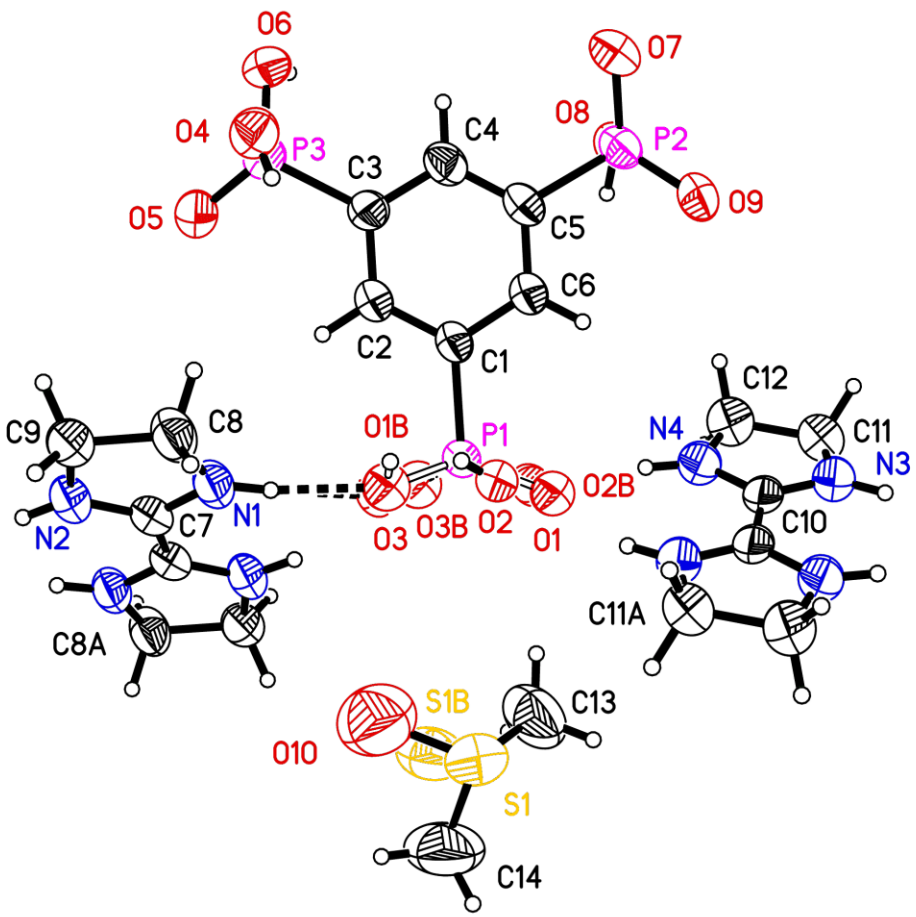

Figure S4. Thermal atomic displacement ellipsoid plot of the structure of crystals of (H_2**BI**$^{+2}$) (H_4**BTP**$^{-2}$) • DMSO grown from DMSO. The ellipsoids of non-hydrogen atoms are drawn at the 50% probability level, and hydrogen atoms are represented by a sphere of arbitrary size. Hydrogen bonds are shown as dotted lines. Atoms labeled with a suffix B are from the second part of the statistically disordered fragments.

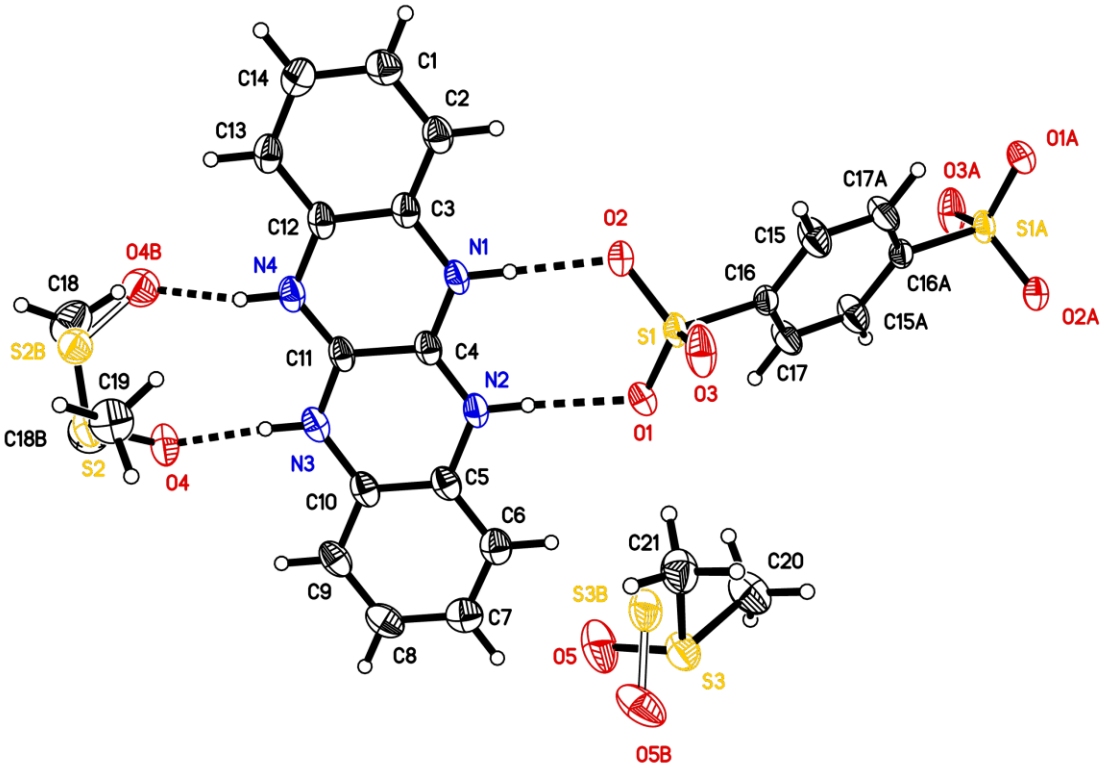

Figure S5. Thermal atomic displacement ellipsoid plot of the structure of crystals of (H**FF**$^{+}$)$_2$ (**BDS**$^{-2}$) • 4DMSO grown from DMSO. The ellipsoids of non-hydrogen atoms are drawn at the 50% probability level, and hydrogen atoms are represented by a sphere of arbitrary size. Hydrogen bonds are shown as dotted lines. Atoms labeled with the suffix A are symmetry-equivalent. Atoms labeled with the suffix B are from the second part of the statistically disordered fragments.

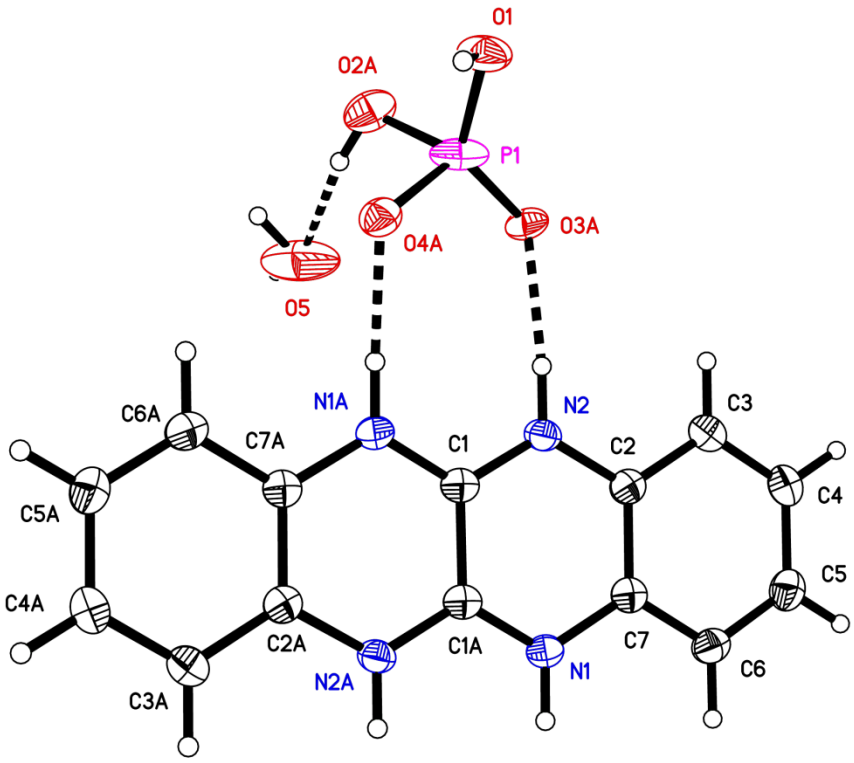

Figure S6. Thermal atomic displacement ellipsoid plot of the structure of crystals of (H_2**FF**$^{+2}$) $[PO_2(OH)_2^-]_2 \bullet H_2O$ grown from heptanoic acid. The ellipsoids of non-hydrogen atoms are drawn at the 50% probability level, and hydrogen atoms are represented by a sphere of arbitrary size. Hydrogen bonds are shown as dotted lines. Only one part of the disordered phosphate anion and water molecule is shown.

X-Ray Powder Diffraction

The experimental patterns were measured on a Bruker D8 Discover diffractometer at 295 K with copper radiation (CuKα, λ = 1.5418 Å). The calculated diffraction patterns were generated from the crystal structure at 100 K or 150 K using Mercury software (http://www.ccdc.cam.ac.uk/products/mercury/).

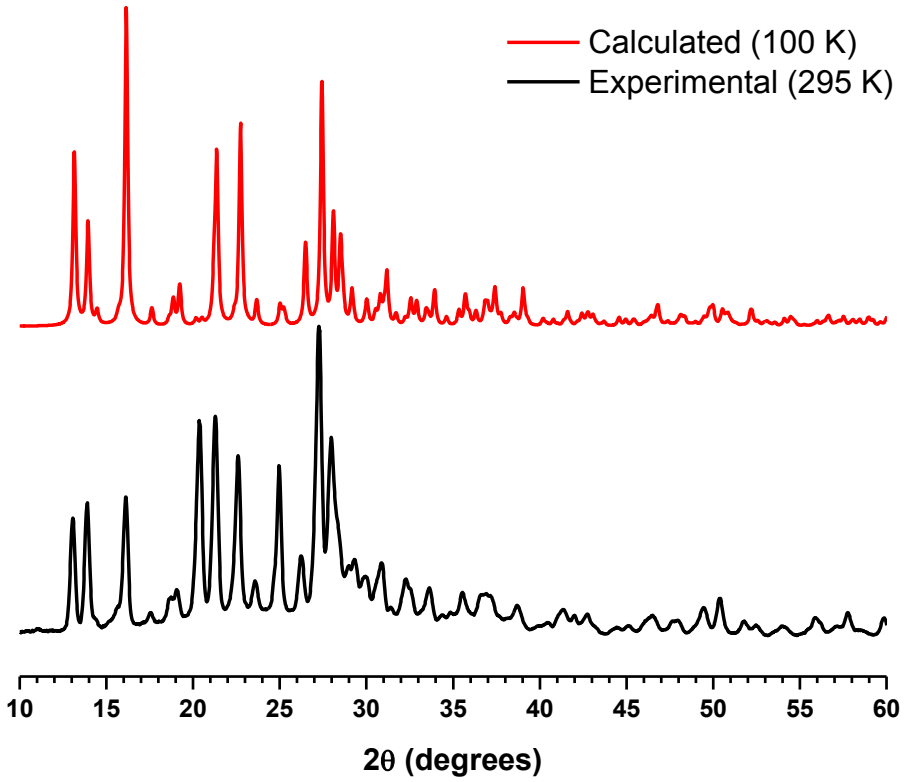

Figure S7. Comparison of calculated and experimental X-ray powder diffraction patterns for crystals of (H_2**BI**$^{+2}$) (H_2**BDP**$^{-2}$) • 4H_2O grown from EtOH/H_2O.

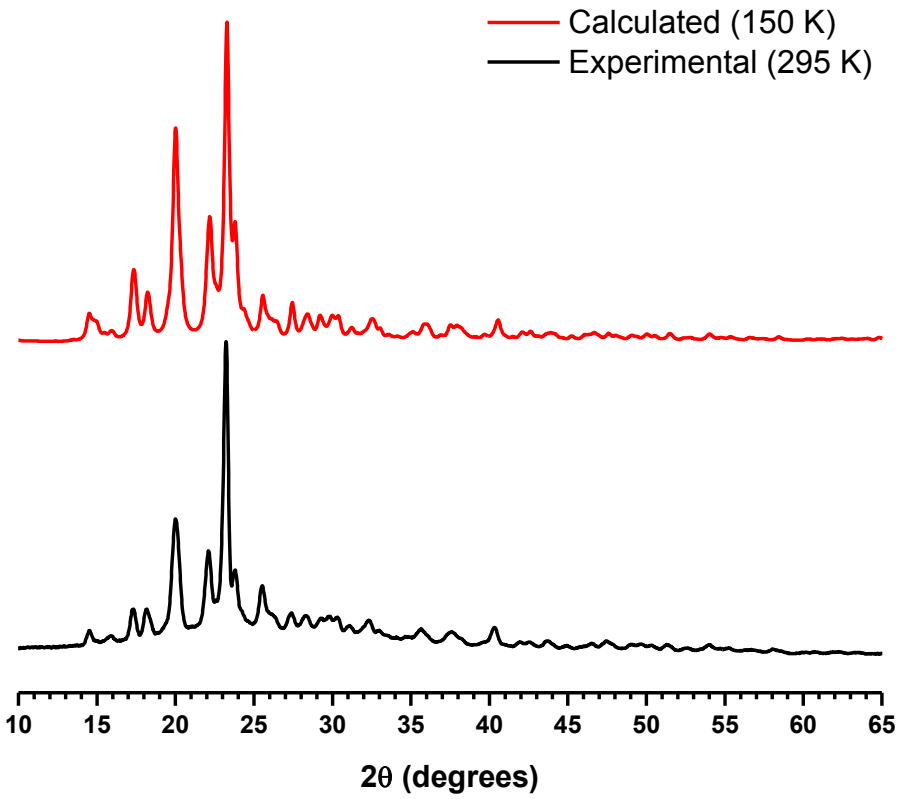

Figure S8. Comparison of calculated and experimental X-ray powder diffraction patterns for crystals of (H_2**BI**$^{+2}$) (H_4**BTP**$^{-2}$) • DMSO grown from DMSO.

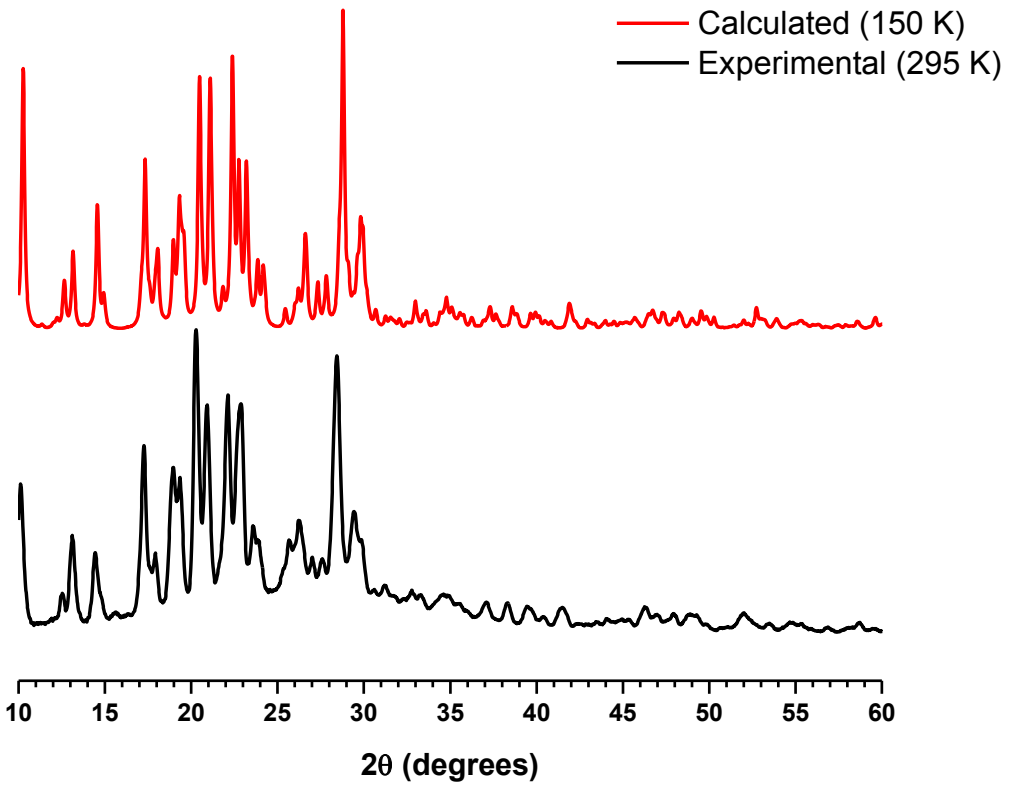

Figure S9. Comparison of calculated and experimental X-ray powder diffraction patterns for crystals of (H**FF**$^{+}$) (**BDS**$^{-2}$) • 4DMSO grown from DMSO.